Check for updates

Received: 30 July 2021 | Revised: 7 December 2021 | Accepted: 24 December 2021

DOI: 10.1111/all.15226

Allergy EUROPEAN JOURNAL OF ALLERGY AND CLINICAL IMMUNOLOGY EAACI WILEY

ORIGINAL ARTICLE

Basic and Translational Allergy Immunology

# Differential effects of lung inflammation on insulin resistance in humans and mice

Ruth Karlina[1,2] | Claudia Flexeder[3,4,5] | Stephanie Musiol[5,6] | Madhumita Bhattacharyya[7] | Evelyn Schneider[5,6] | Irem Altun[1,2] | Silvia Gschwendtner[8] | Avidan U. Neumann[7,9] | Jana Nano[2,3] | Michael Schloter[8] | Annette Peters[2,3] | Holger Schulz[3,5] | Carsten B. Schmidt-Weber[5,6] | Marie Standl[3,5] | Claudia Traidl-Hoffmann[7,9,10] | Francesca Alessandrini[5,6] | Siegfried Ussar[1,2,11]

[1]RG Adipocytes & Metabolism, Institute for Diabetes & Obesity, Helmholtz Zentrum München, Munich, Germany

[2]German Center for Diabetes Research (DZD), Munich, Germany

[3]Institute of Epidemiology, Helmholtz Zentrum München, German Research Center for Environmental Health, Munich, Germany

[4]Institute and Clinic for Occupational, Social and Environmental Medicine, University Hospital, LMU Munich, Munich, Germany

[5]German Center for Lung Research (DZL), Munich, Germany

[6]Center of Allergy & Environment (ZAUM), Technical University of Munich and Helmholtz Zentrum München, German Research Center for Environmental Health, Munich, Germany

[7]Department of Environmental Medicine, Faculty of Medicine, University of Augsburg, Augsburg, Germany

[8]Research Unit for Comparative Microbiome Analysis, Helmholtz Zentrum München, German Research Center for Environmental Health, Neuherberg, Germany

[9]Institute of Environmental Medicine, Helmholtz Zentrum München, German Research Center for Environmental Health, Augsburg, Germany

[10]Environmental Medicine, Technical University Munich, Munich, Germany

[11]Department of Medicine, Technical University of Munich, Munich, Germany

**Correspondence**
Siegfried Ussar, RG Adipocytes & Metabolism, Institute for Diabetes and Obesity, Helmholtz Center Munich, Ingolstädter Landstr. 1, 85764 Neuherberg, Germany.
Email: Siegfried.ussar@helmholtz-munich.de

Francesca Alessandrini, Center of Allergy & Environment (ZAUM), Technical University of Munich and Helmholtz Center Munich, Ingolstädter Landstr. 1, 85764 Neuherberg, Germany.
Email: franci@helmholtz-munich.de

## Abstract

**Background:** The rates of obesity, its associated diseases, and allergies are raising at alarming rates in most countries. House dust mites (HDM) are highly allergenic and exposure often associates with an urban sedentary indoor lifestyle, also resulting in obesity. The aim of this study was to investigate the epidemiological association and physiological impact of lung inflammation on obesity and glucose homeostasis.

**Methods:** Epidemiological data from 2207 adults of the population-based KORA FF4 cohort were used to test associations between asthma and rhinitis with metrics of body weight and insulin sensitivity. To obtain functional insights, C57BL/6J mice were

**Abbreviations:** BAL, bronchoalveolar lavage; BAT, brown adipose tissue; BFMI, body fat mass index; BMI, body mass index; BMR, basal metabolic rate; FACS, fluorescence-activated cell sorting; FFMI, fat-free mass index; HbA1c, hemoglobin A1c; HDM, house dust mites; HFD, high-fat diet; HOMA-IR, homeostasis model assessment-estimated insulin resistance; i.n., intranasal; ILC, innate lymphoid cell; KORA, "Kooperative Gesundheitsforschung in der Region Augsburg" (Cooperative Health Research in the Augsburg Region); LFD, low-fat diet; PBS, phosphate-buffered saline; pgWAT, perigonadal white adipose tissue; scWAT, subcutaneous white adipose tissue; tIgE, total IgE; UCP1, uncoupling protein 1; WAT, white adipose tissue; WHR, waist-to-hip ratio.

Ruth Karlina, Claudia Flexeder, Francesca Alessandrini and Siegfried Ussar equal contribution.

This is an open access article under the terms of the Creative Commons Attribution-NonCommercial-NoDerivs License, which permits use and distribution in any medium, provided the original work is properly cited, the use is non-commercial and no modifications or adaptations are made.
© 2022 The Authors. *Allergy* published by European Academy of Allergy and Clinical Immunology and John Wiley & Sons Ltd.

**Funding information**
The KORA study was initiated and financed by the Helmholtz Zentrum München—German Research Center for Environmental Health, which is funded by the German Federal Ministry of Education and Research (BMBF) and by the State of Bavaria. Mouse studies were supported by the HMGU Allergy Projects from the Helmholtz Center Munich.

intranasally sensitized and challenged with HDM and simultaneously fed with either low-fat or high-fat diet for 12 weeks followed by a detailed metabolic and biochemical phenotyping of the lung, liver, and adipose tissues.

**Results:** We found a direct association of asthma with insulin resistance but not body weight in humans. In mice, co-development of obesity and HDM-induced lung inflammation attenuated inflammation in lung and perigonadal fat, with little impact on body weight, but small shifts in the composition of gut microbiota. Exposure to HDM improved glucose tolerance, reduced hepatosteatosis, and increased energy expenditure and basal metabolic rate. These effects associate with increased activity of thermogenic adipose tissues independent of uncoupling protein 1.

**Conclusions:** Asthma associates with insulin resistance in humans, but HDM challenge results in opposing effects on glucose homeostasis in mice due to increased energy expenditure, reduced adipose inflammation, and hepatosteatosis.

**KEYWORDS**
allergy, house dust mites, inflammation, insulin sensitivity, obesity

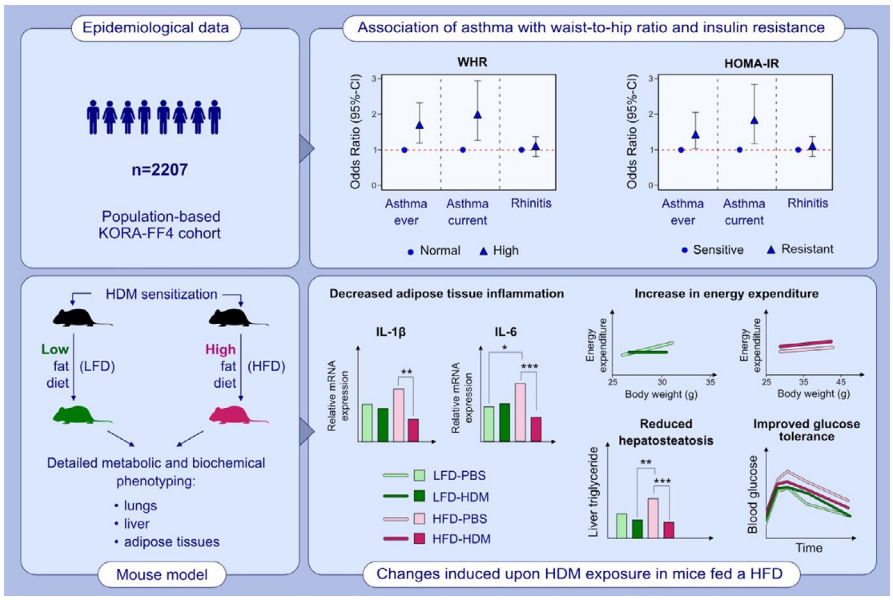


**GRAPHICAL ABSTRACT**
This study investigates the epidemiological association and physiological impact of lung inflammation on obesity and glucose homeostasis. Asthma is associated with increased insulin resistance independently of a body fat mass. HDM-induced lung inflammation increases energy expenditure, decreases adipose tissue inflammation, and hepatosteatosis, resulting in improved glucose tolerance in high-fat diet-induced obese mice.

## 1 | INTRODUCTION

Obesity is a disease of energy imbalance, in which the amount of energy intake is greater than the energy expended.[1] Most obese subjects eventually develop the metabolic syndrome, including insulin resistance, hypertension, hyperlipidemia, and type 2 diabetes, causing increased burden to our health and healthcare system.[2,3] Obesity is a complex, multifactorial disease, dependent on an interaction of genetic predisposition and environmental factors.[4] Based on western lifestyle and increased urban living, the obesity pandemic co-occurs with a steady rise in allergic diseases.[5-7] Today, approximately 30–40% of the population suffers from one or more allergic condition and the prevalence is increasing dramatically in developed and developing countries. Importantly, previous studies identified the metabolic syndrome as a major risk factor for the development of asthma.[8,9] Hersoug and Linneberg hypothesized that the decrease in immunological tolerance induced by obesity results in the increase of allergic diseases.[10] They proposed that the immunological changes induced by adipokines, such as leptin and adiponectin, and cytokines, like IL-6 and TNFα, secreted by white

adipose tissue (WAT) shifts the immune system toward a Th2 cytokine profile and reduces immunological tolerance to antigens (reviewed in[10]). Furthermore, the adipokine leptin was shown to control proliferation of FOXP3$^+$ regulatory T cells[11] and may therefore influence tolerance regulation at the level of the specific immune system.

Conversely, ovalbumin sensitization in mice alleviated diet-induced obesity and metabolic dysfunction by increasing energy expenditure through thermogenic adipose tissue,[12] which in contrast to white fat utilizes energy through mitochondrial uncoupling to generate heat.[13] Thus, a number of studies indicate a connection between allergies and the metabolic syndrome. However, the nature and consequences of this association remain unclear.

One of the major drivers of obesity is a sedentary indoor lifestyle, which in addition to a chronic energy surplus results in continuous exposure to clinically relevant specific aeroallergens, such as house dust mites (HDM).[14] We investigated the epidemiological associations between asthma and rhinitis with metrics of body mass, fat distribution, and insulin sensitivity in 2207 adults, revealing direct associations of asthma with metrics of insulin resistance but not body weight or body fat content in this cohort of subjects averaging 60 years of age. To obtain mechanistic insights into these associations, we designed a study mimicking the simultaneous exposure to low-fat (LFD) or high-fat diet (HFD) feeding and HDM extract using male C57BL/6J mice. We conducted a detailed metabolic and immunological characterization of key metabolic organs, gut microbiota, and the lung to show that the prolonged exposure to HDM and HFD does not impair body weight gain, but induces small yet significant shifts in the composition of gut microbiota. Conversely, co-exposure of HDM and HFD attenuated inflammation in lungs and perigonadal WAT (pgWAT), as well as increases energy expenditure through browning of subcutaneous WAT (scWAT) and brown adipose tissue (BAT), resulting in an overall improvement in glucose metabolism. Thus, humans and mice show opposing effects on glucose homeostasis upon allergic lung inflammation, which could be explained by differences in amount and activity of BAT.

## 2 | MATERIALS AND METHODS

### 2.1 | Epidemiological data analysis

The KORA study was approved by the respective ethics committee of the Bavarian Medical Association. The investigations were carried out in accordance with the Declaration of Helsinki. All participants gave written informed consent.

#### 2.1.1 | Study population

The present analysis is based on a follow-up study of the fourth survey of the population-based KORA S4 (Cooperative Health Research in the Augsburg Region) cohort comprising 4,261 adults recruited in 1999-2001. The KORA FF4 follow-up study comprises 2,279 study participants, examined between 2013 and 2014. The primary study design has been described previously in more detail.[15,16]

#### 2.1.2 | Exposure and outcome assessment

Different obesity and body composition measures were used as exposure variables. Data on height, weight, waist and hip circumference, and body impedance measurement were collected in a standardized physical examination. Body weight was measured in light clothes and without shoes to the nearest 0.1 kg and height to the nearest 0.1 cm. Body mass index (BMI) was calculated as the ratio of weight in kilogram to height in meter squared. Waist circumference was measured at the level midway between the lower rib margin and the iliac crest, and hip circumference was measured at the widest point over the greater trochanters, both to the nearest 0.1 cm. Waist-to-hip ratio (WHR) was calculated as the ratio of waist and hip circumference and categorized into normal vs. high with cutoffs ≥1 for males and ≥0.85 for females [see eg,[17]]. Fat-free mass (FFM) and body fat mass (BFM) were measured by bioelectrical impedance analysis using the BIA 2000-S device (Data Input, Pöcking, Germany) with an operating frequency of 50 kHz at 0.8 mA. Ohmic resistance was measured at the dominant hand (between wrist and dorsum) and the dominant foot (between angle and dorsum).[18] Fat-free mass and body fat mass were then calculated by means of Kyle's equations[19] and fat-free mass index (FFMI, ratio of fat-free mass in kg and height in meter squared) and body fat mass index (BFMI, ratio of body fat mass in kg and height in meter squared) were derived.

Fasting glucose, fasting insulin, and hemoglobin A1c (HbA1c) were assessed in fasting blood samples. HbA1c was measured in whole blood using the cation-exchange high-performance liquid chromatographic, photometric Variant II Turbo HbA1c Kit-2.0 assay on a Variant II Turbo Hemoglobin Testing System (Bio-Rad Laboratories Inc.). Glucose levels were measured in serum using an enzymatic colorimetric method on a Dimension Vista 1500 instrument (Siemens Healthcare Diagnostics Inc.) or the GLUC3 assay on a Cobas c702 instrument (Roche Diagnostics GmbH). Insulin levels were measured in serum using an eletrochemiluminescence immunoassay on a Cobas e602 instrument (Roche) or a solid-phase enzyme-labeled chemiluminescent immunometric assay on Immulite 2000 systems analyzer (Siemens). Homeostasis model assessment of insulin resistance (HOMA-IR) was calculated as (fasting insulin [mU/L] × fasting glucose [mmol/L]/22.5).[18,20,21]

HOMA-IR was categorized into insulin sensitive (HOMA-IR <2.5) and insulin resistant (HOMA-IR ≥2.5) whereas HbA1c was categorized into normal (HbA1c <5.7%), prediabetes (HbA1c ≥5.7% and <6.5%), and diabetes (HbA1c ≥6.5%).[22,23]

Doctor-diagnosed asthma and rhinitis were defined as affirmative answers to the question "Have you ever been diagnosed with asthma by a physician?" and "Have you ever been diagnosed with hay fever by a physician?" requested by the participants via questionnaire at the corresponding study follow-up. The participants were also asked whether they had wheezing or whistling in the chest during the past

12 months and whether they are currently taking any asthma medication. Current asthma was then defined as fulfilling at least two out of the following three criteria: ever doctor-diagnosed asthma, wheezing within the last 12 months, and current asthma medication.

#### 2.1.3 | Statistical analyses

All analyses were performed using the statistical software package R, version 4.0.3 [R Core Team. R: A Language and Environment for Statistical Computing. Vienna, Austria; 2020. Available from: https://www.R-project.org/]. Mean and corresponding standard deviation (SD) or percentages and frequencies (%, *n*/*N*) were used to describe study characteristics. Differences between groups were tested using Pearson's chi-squared test for categorical variables and *t*-test for continuous variables. Observations exceeding mean ± 4 SD were considered as outliers and excluded from further analyses. Due to the skewed distribution, the continuous HOMA-IR variable was log-transformed (natural logarithm).

Adjusted logistic regression models were used to analyze the association between obesity and body composition measures with allergic diseases. The models were adjusted for sex, age, smoking status, education level, physical activity, alcohol consumption, and hypertension. Smoking status was categorized as never, former, and current smoker, education level was categorized as low (<10 years of school), medium (10 years of school), and high (>10 years of school), and physical activity was categorized as no activity, low activity (irregular about 1 h/week), moderate activity (regular about 1 h/week), and high activity (regular more than 2 h/week). Alcohol intake was categorized as no intake (0 g/day), low intake (>0–<40 g/day for males and >0–<20 g/day for females), and moderate intake (≥40 g/day for males and ≥20 g/day for females). In addition, models with mutual adjustment of obesity and body composition measures (BMI, BFMI, FFMI, and WHR) with HOMA-IR and HbA1c were calculated. All regression models were also stratified by sex. Interaction terms between measures of obesity with HOMA-IR and HbA1c were tested. As none of the interaction terms reached significance, the regression models have not been further stratified. In total, 2207 study participants were included in the current analysis with complete information on allergic diseases, measures of obesity (BMI, BFMI, FFMI, and WHR), and covariates.

### 2.2 | Mice

C57BL/6J male mice were obtained from Charles River (Sulzfeld, Germany) and kept under specific pathogen-free conditions in individually ventilated cages (IVC) at constant ambient temperature of 22 ± 2°C, 45–65% humidity, a 12 h light-dark cycle, with *ad libitum* access to food and water. Mice were fed either a HFD containing 58 kcal% fat, 25.5 kcal% carbohydrates, and 16.4 kcal% proteins (D-12331, Research Diets, New Brunswick, NJ, USA) or a LFD containing 10.5 kcal% fat, 73.1 kcal% carbohydrates, and 16.4 kcal% proteins (D-12329, Research Diets). Neither of the diets contained a significant amount of fiber. Mice were grouped to have equal mean starting body weight in each group and sensitized by bilateral intranasal (i.n.) instillations of 1μg of *Dermatophagoides farinae* extract (HDM, Citeq Biologics, Groningen, NL) in 20μl PBS. After 7 days, mice were challenged for 5 consecutive days and thereafter every other week until the end of the experiment by bilateral i.n. instillations of 10μg of the same HDM extract in 20μl PBS. Control animals received the same amount of PBS. Mice were sacrificed 72h after the last i.n. instillation. Prior to sacrifice, glucose and insulin tolerance tests were performed in week 9 and 10, respectively and body composition was analyzed with a non-invasive magnetic resonance whole body composition analyzer (EchoMRITM) in week 11. Cumulative food and water intake, locomotor activity, respiratory quotient and energy expenditure were measured in individually-housed mice for 5 consecutive days in week 11 with an indirect calorimetric system (TSE PhenoMaster). Animal experiments were conducted under permission according to the German animal welfare law, relevant guidelines and regulations of the government of Upper Bavaria (Bavaria, Germany): ROB-55.2-2532.Vet_02-18-94 and ROB-55.2-2532.Vet_02-14-172.

### 2.3 | Glucose and insulin tolerance test

Mice were fasted for 4 h prior to glucose and insulin tolerance test. Glucose (2 g/kg body weight, 20% glucose solution, B. Braun) was injected intraperitoneally (i.p.) to the mice for glucose tolerance test (GTT). Insulin (Actrapid, Novo Nordisk) was administered i.p. with a dose of 0.75 IU insulin/kg body weight for the LFD group and 1.25 IU insulin/kg body weight for the HFD group. Glucose levels were measured from the blood collected from the tail before (0 min), 15, 30, 60, and 120 min after injection, using a glucometer (Abbott).

### 2.4 | Measurement of serum immunoglobulins, serum metabolites, and liver triglycerides

Serum total IgE was measured by ELISA as previously described.[24] Insulin concentration was analyzed using mouse ultrasensitive insulin ELISA kit (CrystalChem). Liver triglyceride content was quantified using Triglyceride Quantification Colorimetric Kit (BioVision).

### 2.5 | Analysis of bronchoalveolar lavage (BAL) fluid

After sacrifice, all lungs were subjected to bronchoalveolar lavage (BAL). Total and differential BAL cell counts were calculated as previously described.[24] For cytokine analysis, a mouse Th Cytokine Panel LEGENDplex™ (BioLegend®) was used according to the manufacturer's instructions. Concentration of the analytes was determined based on a known standard curve using data analysis software LEGENDPlex™ version v8.0 provided by the manufacturer.

## 2.6 | Tissue histology

Lung, adipose tissue, and liver were fixed in 4% PFA/PBS at 4°C overnight and embedded in paraffin. Adipose tissues and liver were cut 2 μm thick and stained with hematoxylin and eosin. Lung sections (3–4 μm thick) were stained with periodic acid and Schiff reagent (PAS). Mucus hypersecretion and inflammatory cell infiltration were graded in a blinded fashion on a scale from 0 to 4 (0: none, 1: mild, 2: moderate, 3: marked, and 4: severe), reflecting the degree of the pathological alteration.[24] Pictures were taken with transmitted light imaging microscope (Axioscope 5).

## 2.7 | Isolation and analysis of leukocytes from lungs

Lungs were digested in RPMI medium supplemented with 100 μg/ml DNAse (Sigma-Aldrich) and 1 mg/ml Collagenase type 1A (Sigma-Aldrich) at 37°C for 20 min. Digested lungs were filtered through a 70 μm cell strainer and centrifuged at 400 G and 4°C for 5 min. Pellets were resuspended in a gradient of 40% Percoll® in RPMI (v/v) solution and 80% Percoll® solution (GE Healthcare-Life Sciences). Tubes were centrifuged at room temperature and 1600 G for 15 min with brake set to 0. Lymphocytes were collected from the interphase and analyzed via fluorescence-activated cell sorting (FACS). Single cell suspensions were primarily stained with surface markers. Cells were stained for transcription factors using Foxp3 Staining Buffer Set (eBiosciences) according to the manufacturer's protocol and analyzed using BD LSRII Fortessa flow cytometer (BD Bioscience) and FlowJo Software (FlowJo). Antibodies that were used for flow cytometry purposes are listed in Table S4, and the gating strategy employed for the analysis is depicted in Figure S3A.

## 2.8 | Protein extraction and western blot

Brown adipose tissue was lysed in RIPA buffer (50 mM Tris pH 7.5, 150 mM NaCl, 1 mM EDTA, 1% Triton X-100), containing 0.1% SDS, 1% protease-inhibitor, 1% phosphatase-inhibitor cocktail II, and 1% phosphatase-inhibitor cocktail III (all from Sigma). Protein concentrations were measured using BCA Protein Assay Kit (Thermo Fischer Scientific). Proteins were separated by SDS-PAGE and transferred to a PVDF membrane (Merck Millipore). Unspecific binding sites were blocked with 5% milk/TBS-T. Membranes were incubated with Ucp1 antibody (Abcam cat# ab10983) with dilution 1:1000. The following day, membranes were washed with PBS and incubated with secondary HRP-conjugated antibody (Cell Signaling Technology cat# 7074) with 1:5000 dilutions. α-tubulin (Santa Cruz Biotechnology, Sc-8035) and Gapdh (6C5, Merck Millipore) were used as loading control with dilution 1:5000. Prior to imaging, membranes were washed with TBS-T and developed with ChemiDoc™ (Bio-Rad). Quantification of band intensities was analyzed in Image Lab Software (Bio-Rad).

## 2.9 | RNA extraction and qPCR

Qiazol (Qiagen) and metal beads were added to the frozen tissues in order to disrupt and homogenize the tissues in TissueLyser II (Qiagen). Samples were then centrifuged and chloroform was added to the lysate to create a phase separation. After another centrifugation step, the clear lysate was collected and a volume of 70% ethanol was added to the lysate. RNA extraction procedure then continued using a spin column according to the protocol of RNeasy Mini Kit (Qiagen). Total RNA concentration and purity were determined by spectrophotometer at 260 nm (NanoDrop 2000 UV-Vis Spectrophotometer; Thermo Scientific). RNA (500 ng) was converted to cDNA using the High-Capacity cDNA Reverse Transcription Kit (Applied Biosystems). Semi-quantitative qPCR was performed using iTaq™ Universal SYBR® Green Supermix (Bio-Rad) in a CFX384 Touch Real-Time PCR Detection System (Bio-Rad) with primers listed in Table S5. Relative mRNA expression was calculated after normalization to TATA-binding protein (Tbp), unless indicated otherwise in the figure legend.

## 2.10 | Gut *microbiota* profiling: sampling and 16S rRNA gene library preparation

*Fecal* materials were snap frozen in liquid nitrogen and stored at −80°C until processing. DNA was extracted from each probe using phenol-chloroform extraction[25] with the following modification: feces were pre-incubated with 750 μl $NaPO_4$ and 250 μl TNS for 30 min at 55°C. After extraction, DNA was resolved in nuclease-free water.

Amplicon sequencing of the V1–V2 hypervariable region of the 16S rRNA gene was performed on a MiSeq Illumina (Illumina) using the universal eubacterial primers 27f 5′-AGAGTTTGATCMTGGC-3′, and 357r 5′-CTGCTGCCTYCCGTA-3′,[26] extended with sequencing adapters to match Illumina indexing primers. The protocol was described in detail by Alessandrini et al.[27] Briefly, sequencing PCR (98°C for 1 min, followed by 20 cycles of 98°C for 10 s, 60°C for 30 s, 72°C for 30 s, and final extension at 72°C for 5 min) was performed in technical triplicates using 1× NebNext High Fidelity Mastermix (New England Biolabs), 0.5 mM of each primer, and 5 ng of template DNA (25 μl total volume). To exclude potential contamination, blank extraction and PCR control without template DNA were processed additionally. PCR products were visualized on 1% agarose gel. Afterward, PCR triplicates were pooled, purified via AMPure beads XP (Beckman Coulter), and quantified with a Fragment Analyzer using the DNF-473 NGS Fragment Kit (Agilent). For indexing PCR (98°C for 30 s, followed by eight cycles of 98°C for 10 s, 55°C for 30 s, 72°C for 30 s, and final extension at 72°C for 5 min), 10 ng of template DNA, 1× NebNext High Fidelity Mastermix (New England Biolabs), and indexing primer 1 (N7xx) and indexing primer 2 (S5xx) were used (25 μl total volume). After purification via AMPure beads XP, the PCR products were validated via Fragment Analyzer using

the DNF-473 NGS Fragment Kit (Agilent, Santa Clara, CA, USA) and pooled to a final concentration of 4 nM for the MiSeq sequencing run, which was performed using MiSeq Reagent Kit v3 (600 Cycle) (Illumina).

### 2.11 | Microbiome data acquisition and analysis

Microbiome sequencing data were processed following the DADA2 (version 1.16.0) pipeline[28] in R (version 3.6.4). Briefly, the data were filtered, that is, adapter, barcode, and primer clipped, and the ends of sequences with high numbers of errors were trimmed. The amplicons were denoised based on a model of the sequencing errors, and paired-end sequences were merged. Sequences with <200 base pairs and chimeric sequences were discarded. The resulting amplicon sequence variants (ASV) were annotated using the AnnotIEM in-house software that compares sequence alignment against four databases EzBioCloud,[29] NCBI,[30] RDP,[31] and Silva.[32] Singletons (only one read present per sample), contaminants (as identified by dominance in negative controls), and eukaryotic ASVs were removed from downstream analysis for additional quality control. The final microbiome data set comprised of 2179974 reads (median per sample 53,461; range 32,471–2,51,493) that were assigned to 836 ASVs (median per sample 287; range 74–422). All statistical analyses were performed using the statistical software package R (version 4.0.3). Additionally, MicrobiomeAnalystR package[33] was used for advanced analysis and data visualization. All analyses were performed on the ASV level and read counts per sample were normalized by total sum scaling (TSS) method as required in order to be comparable. Statistical comparison between groups was performed using non-parametric Kruskal–Wallis test; raw *p*-values ≤0.05 from two-sided tests were considered statistically significant. Beta diversity was estimated by pairwise ecological distances between samples using Bray–Curtis dissimilarities and visualized by PCoA. Statistical significance between groups was assessed using a permutational analysis of variance (PERMANOVA) test with 1000 permutations. Taxonomic distributions are shown using stacked bar plots for which ASVs with identical taxonomy were summarized into family. The 10 most frequent families were selected by mean relative abundance over all samples, and the remaining species were summarized as "Others."

### 2.12 | Statistical analysis for mouse experiments

Data are shown as mean +/- standard error mean (SEM), if not indicated otherwise. Statistical significance for multiple comparisons was determined by One- or Two-Way ANOVA, with Tukey's multiple comparisons test, or unpaired t-test (two-tailed P value). Correlation graphs were analyzed with linear regression (two-tailed P value, 95% CI). GraphPad Prism 6 was used for statistical analysis. P values <0.05 were considered as statistically significant.

## 3 | RESULTS

### 3.1 | Asthma and rhinitis directly associate with metrics of insulin sensitivity but not with body fat content

To study the epidemiological association between allergic lung inflammation and metrics of the metabolic syndrome, we used data from the KORA FF4 follow-up study.[15,16] The study population consisted of 2207 (48.1% male) subjects. Of those, 8.6% ever had a doctor diagnosis of asthma, 5.3% currently had asthma, and 18.6% had rhinitis (Table S1). The prevalence of asthma was higher among females compared to males (10.0% vs. 7.2% for asthma ever). Study participants had on average a body mass index (BMI) of 27.7 kg/m², a body fat mass index (BFMI) of 9.3 kg/m², and a fat-free mass index (FFMI) of 18.4 kg/m². About 40% of the subjects had a high waist-to-hip ratio (WHR) (≥1 for males and ≥0.85 for females, respectively), and about 40% were classified as insulin resistant based on a homeostasis model assessment-estimated insulin resistance (HOMA-IR) of at least 2.5. Using hemoglobin A1c (HbA1c) as diagnostic marker, 21.5% were prediabetic (HbA1c ≥5.7% but <6.5%) and 5.9% diabetic (HbA1c ≥6.5%; Table S1). Regression models for the association between measures of obesity, body composition, and insulin sensitivity with allergic diseases did not show an association of BMI and BFMI with asthma or rhinitis (Figure 1). However, we observed an inverse association between FFMI and rhinitis (odds ratio [OR]: 0.92; 95% confidence interval [CI]: 0.87–0.98). Interestingly, we found a direct association of WHR with asthma. Those with a high WHR had 1.7 times higher odds of ever having asthma compared to those with normal WHR (OR: 1.66; 95%-CI: 1.19–2.32). Furthermore, those being classified as insulin resistant according to a HOMA-IR of at least 2.5 also had a higher risk for ever having a doctor diagnosis of asthma (OR: 1.45; 95%-CI: 1.03–2.05; Figure 1). Similar associations were observed for current asthma. The direct association between HOMA-IR and asthma remained statistically significant after additional adjustment for BMI, BFMI, and FFMI (Table S2). However, if WHR and HOMA-IR were included in the model at the same time, only WHR showed a statistically significant association with asthma (Table S2). The direct and significant association between WHR and HOMA-IR with asthma also remained when additionally adjusting for HbA1c (Table S3). Interestingly, we observed an inverse association with rhinitis and type 2 diabetes. These data suggest that asthma but not rhinitis, independently of body fat mass, associates with increased insulin resistance. The models stratified by sex showed comparable results between males and females regarding effect direction (Figure S1). However, a significant and direct association between WHR and asthma could only be observed for females (asthma ever: OR 1.97; 95%-CI 1.27–3.06 and current asthma: OR 1.95; 95%-CI 1.11–3.43) but not for males (asthma ever: OR 1.23; 95%-CI 0.69–2.19 and current asthma: OR 1.87; 95%-CI 0.95–3.69).

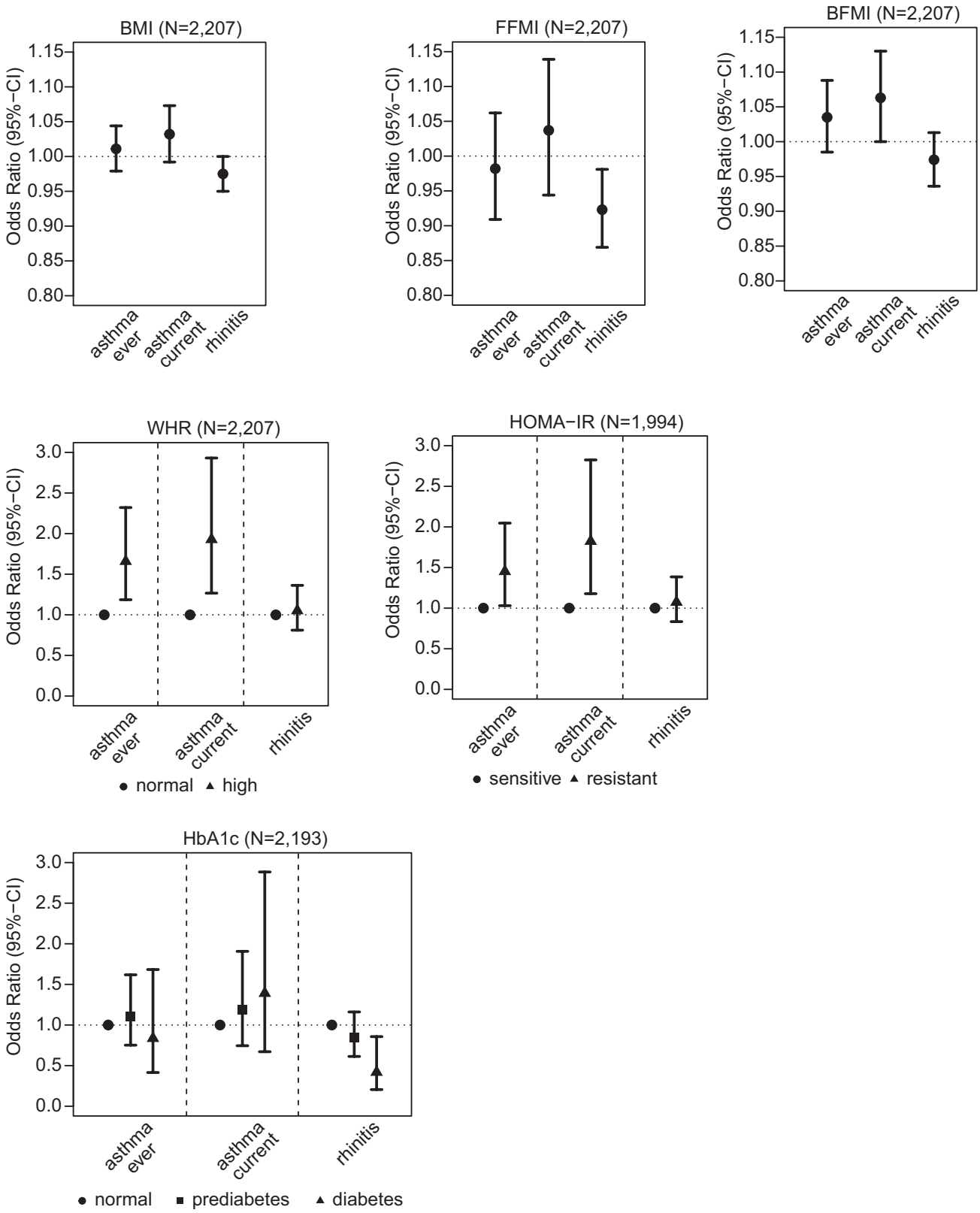


**FIGURE 1** Epidemiological association between asthma and rhinitis with metrics of body fat content and insulin sensitivity. Logistic regression models were adjusted for age, sex, smoking status, education level, physical activity, alcohol consumption, and hypertension. Current asthma is defined as fulfilling at least two out of the following three criteria: ever doctor-diagnosed asthma, wheezing within the last 12 months, and current asthma medication. WHR is defined as normal vs. high with cut-off ≥1 for males and ≥0.85 for females. HOMA-IR is categorized into insulin sensitive (HOMA-IR <2.5) and insulin resistant (HOMA-IR ≥2.5) whereas HbA1c is categorized into normal (<5.7%), prediabetes (≥5.7% and <6.5%), and diabetes (≥6.5%). Results are presented as odds ratios (OR) with corresponding 95% confidence interval (CI)

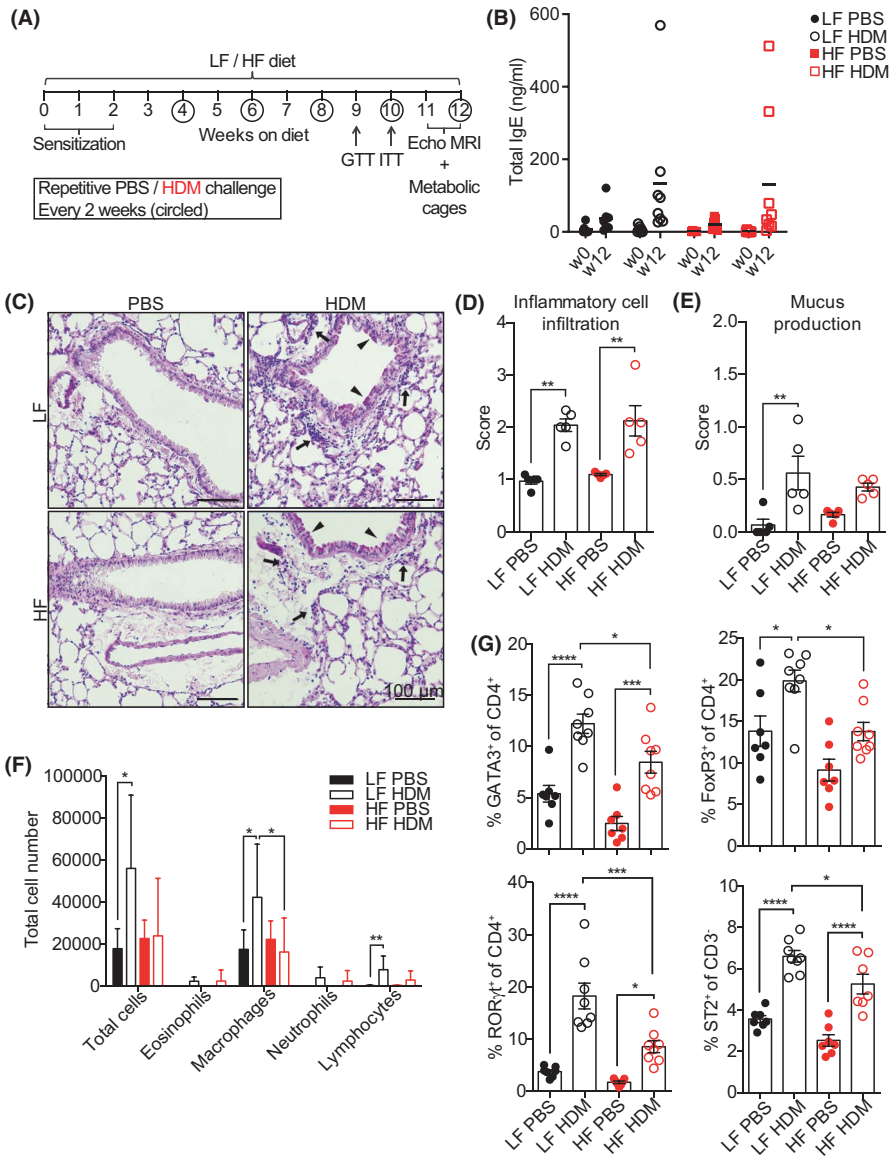


**FIGURE 2** Attenuated immune response in the lungs upon HDM exposure in HFD-fed mice. (A) Experimental setup of repetitive PBS or HDM exposure along with LFD or HFD feeding. (B) Total serum IgE measured at the beginning (week 0) and at the end (week 12) of experiment ($n = 7–8$). (C) Representative PAS staining of lung sections from mice repetitively exposed to PBS or HDM and fed with LFD or HFD (arrows: inflammatory infiltrate; arrowheads: mucus hypersecretion; scale bar: 100 µm). Scoring of (D) inflammatory cell infiltration and (E) mucus production from (C), ($n = 5$). (F) Total BAL cell counts of mice exposed to PBS or HDM and fed with LFD or HFD ($n = 7–8$). (G) Flow cytometric analysis of lung tissue ($n = 7–8$). Mean ± SEM; one- (Figure 2D–G) or two-way (Figure 2B) ANOVA with Tukey's multiple comparisons test. $^{*}p < 0.05$; $^{**}p < 0.01$; $^{***}p < 0.001$; $^{****}p < 0.0001$

## 3.2 | High-fat diet feeding attenuates allergic lung inflammation in response to house dust mite allergen

To mechanistically dissect the interconnection between metabolic disease and allergic lung inflammation, C57BL/6J mice were fed either a low (LFD) or high-fat (HFD) diet for 12 weeks and concomitantly sensitized and repeatedly challenged with HDM (Figure 2A). Repeated HDM exposures following an initial sensitization protocol maintained a mild allergic lung inflammatory response characterized by slightly elevated tIgE levels at the end of experiment (Figure 2B) and increased perivascular and peribronchiolar inflammatory cell infiltration and mucus hypersecretion in both HDM-treated groups (Figure 2C–E). BAL cell analysis revealed significantly increased total cell number in the LFD HDM group (11,200 vs 55,873), but not in the HFD group compared to the PBS control (22,643 vs 23,911; $p = 0.9996$). BAL differential cell count revealed alveolar macrophages and lymphocytes to be responsible for this increase. However, regardless of the diet, also eosinophils and neutrophils were slightly increased in the HDM groups (Figure 2F). Evaluation of BAL Th1/Th2/Th17 and pro-inflammatory cytokines revealed a slight increase of almost all cytokines following allergen challenge, regardless of diet, although not reaching significance (Figure S2).

To further characterize the type of lung immune response in our experimental setting, we performed FACS analysis of lung tissue (Figure S3A). Although no changes in lung resident $CD4^{+}$ and $CD8^{+}$ cells were found (Figure S3B), we observed a relative increase in the percentage of $GATA3^{+}$ (5.7% vs 12.2%), $FoxP3^{+}$ (14.6% vs 19.9%), as well as $ROR\gamma t^{+}$ (4.2% vs 18.3%), and $ST2^{+}$ (3.6% vs 6.6%) cells in LFD-fed HDM-exposed mice compared to PBS controls (Figure 2G). Similar results were also observed in HFD-fed mice, albeit the relative percentage of these cell types following HDM challenge was significantly reduced compared to HDM-challenged LFD-fed animals [$GATA3^{+}$ (12.22% vs 8.5%), $FoxP3^{+}$ (19.9% vs 13.8%), $ROR\gamma t^{+}$ (18.3% vs 8.6%), and $ST2^{+}$ (6.6% vs 5.3%)] (Figure 2G). Thus, consumption of HFD reduced the

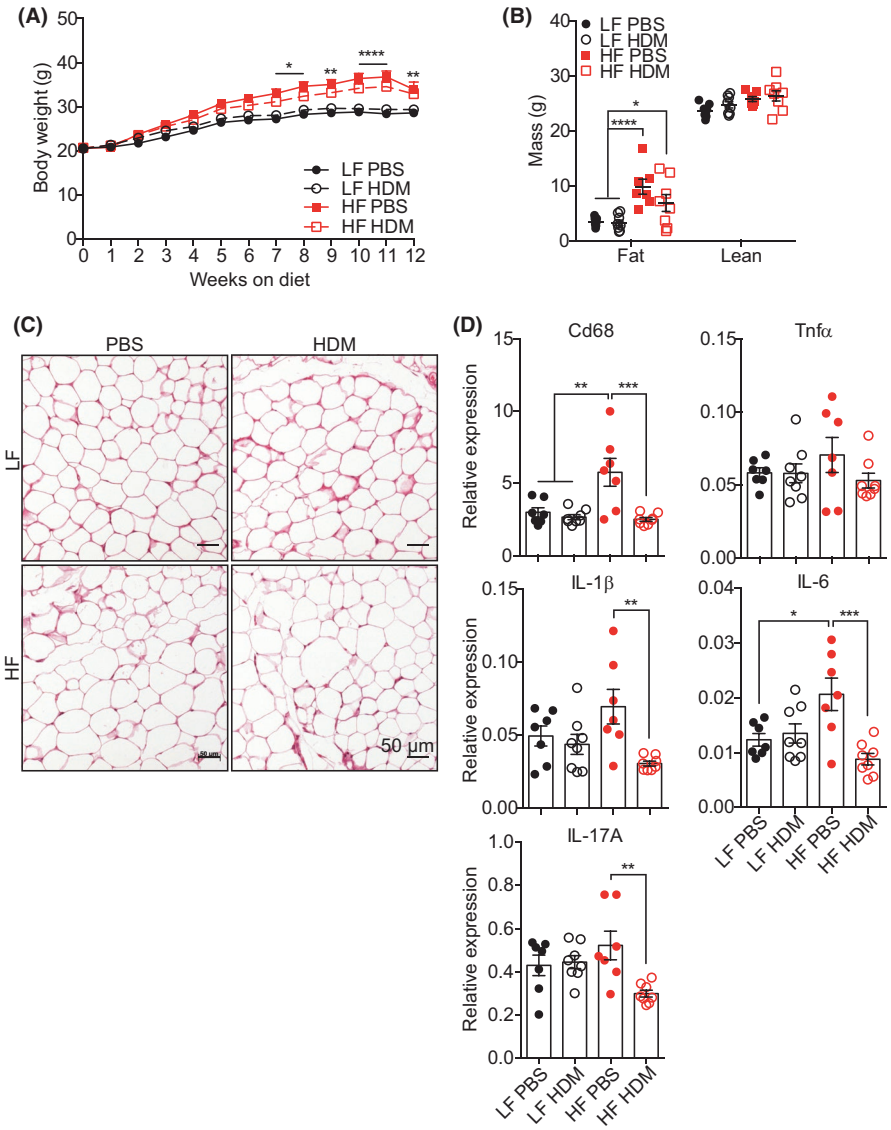


**FIGURE 3** HDM exposure reduced HFD-induced fat mass gain and pgWAT inflammation. (A) Body weight curves and (B) body composition of mice upon constant exposure to PBS or HDM and LFD or HFD ($n = 7–8$). (C) Representative image of H&E staining, (D) relative mRNA levels of Cd68, Tnfα, IL-6, IL-1β, and IL-17A ($n = 7–8$) from mice repetitively exposed to PBS or HDM and fed with LFD or HFD. Mean ± SEM; one-way ANOVA with Tukey's multiple comparisons test. $^{*}p < 0.05$; $^{**}p < 0.01$; $^{***}p < 0.001$; $^{****}p < 0.0001$

abundance of selected immune cell populations, overall dampening HDM-induced lung allergic inflammation compared to LFD.

### 3.3 | Sensitization to HDM in HFD-fed mice has no net effects on body weight and reduces inflammation in the perigonadal white adipose tissue

LFD-fed mice gained an average of 8.1 g during the 12-week study, with no statistical differences between HDM-exposed and control mice [7.4 ± 1.1 g (control), 8.8 ± 0.2 g (HDM)]. HFD-fed mice gained more body weight (12.8 ± 1 g vs 8.1 ± 0.6 g) than LFD-fed mice, which became significant after 6 weeks. We did not observe statistically significant differences between HDM and control-treated HFD-fed mice [13.4 ± 1.3 g (control), 12.2 ± 0.7 g (HDM)] (Figure 3A). Analysis of body composition by Echo-MRI showed no differences in lean mass between groups, but, as expected, HFD-fed mice had significantly more fat mass than LFD-fed mice (8.4 ± 1.5 g vs 3.3 ± 0.5 g; $p = 0.0005$; Figure 3B). HFD-fed HDM mice showed a trend for decreased fat mass compared to PBS controls (6.9 ± 1.5 g vs 9.8 ± 1.4 g; $p = 0.1444$), albeit this did not reach statistical significance. Similarly, we observed a trend for reduced pgWAT mass (Figure S4, left; $p = 0.586$) in HFD-fed HDM mice. Thus, repeated exposure to HDM had no major impact on body weight development. These data were confirmed by histological analysis of pgWAT, which did not show differences in adipocyte size, fibrosis, or the formation of crown-like structures (Figure 3C) in HDM-treated mice compared to their respective diet controls.

A hallmark of diet-induced obesity and one of the underlying causes for the induction of systemic insulin resistance and glucose intolerance is adipose tissue, especially visceral adipose tissue inflammation.[34]

We therefore analyzed several inflammatory markers in pgWAT. Expression of the pan macrophage marker Cd68 was reduced by 3.3% ($p = 0.0007$) in HDM-treated HFD-fed mice, compared to the PBS controls (Figure 3D), while no differences were observed in LFD-fed mice. In line with this, we found a reduced expression of the M1 macrophage markers IL-6, IL-1β and to a lesser extent Tnfα

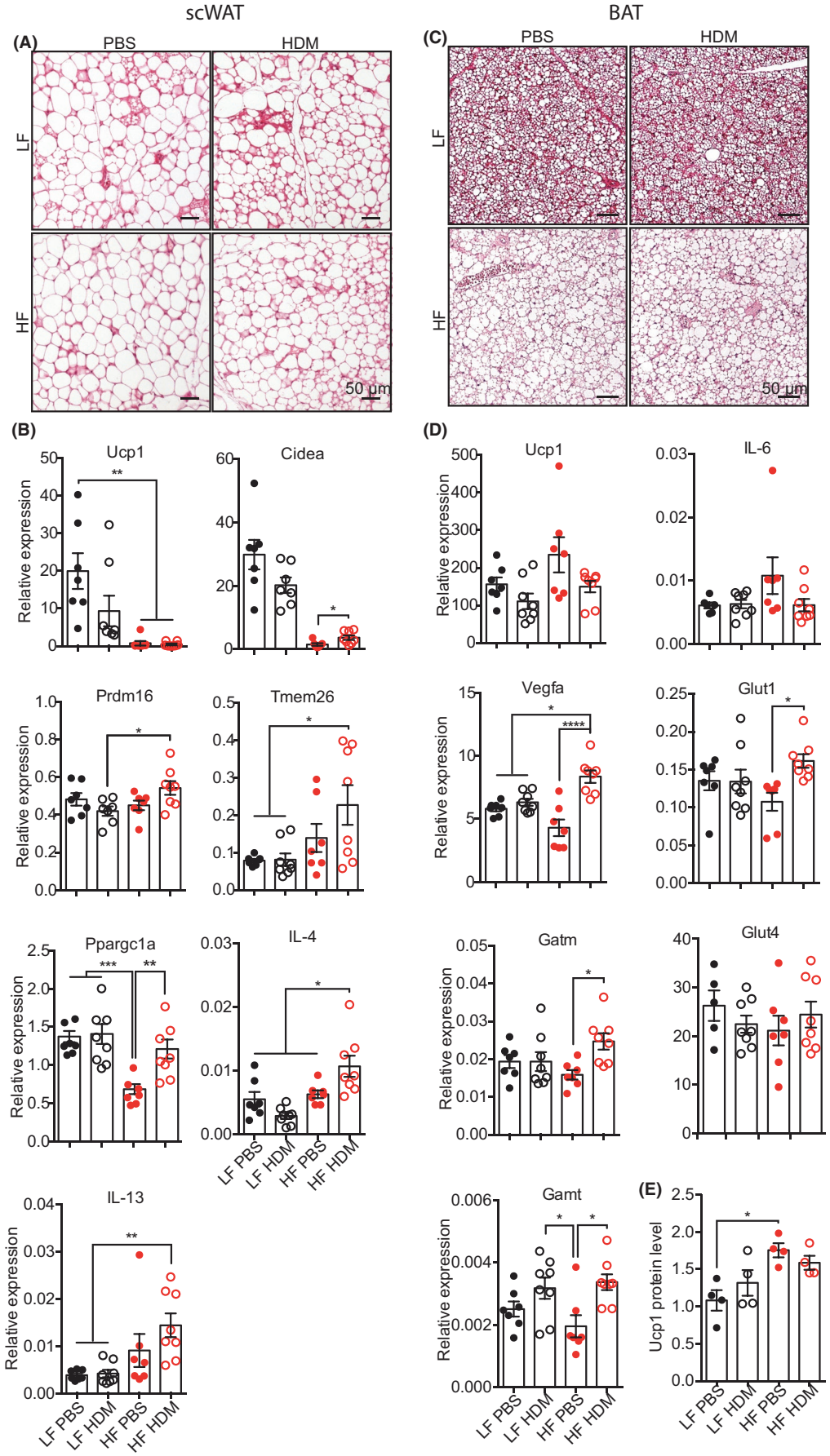
scWAT
BAT
(A)
PBS
HDM
LF
HF
50 μm
(C)
PBS
HDM
LF
HF
50 μm
(B)
Ucp1
Cidea
Prdm16
Tmem26
Ppargc1a
IL-4
IL-13
Relative expression
LF PBS
LF HDM
HF PBS
HF HDM
(D)
Ucp1
IL-6
Vegfa
Glut1
Gatm
Glut4
Gamt
Relative expression
(E)
Ucp1 protein level

**FIGURE 4** HFD-fed mice show an increase in beiging markers in scWAT and BAT upon HDM exposure. (A) Representative image of H&E staining and (B) relative mRNA expression of Ucp1, Cidea, Prdm16, Tmem26, Ppargc1a, IL-13, and IL-4 from scWAT ($n$ = 7–8) of mice repetitively exposed to PBS or HDM and fed with LFD or HFD. (C) Representative images of H&E staining in BAT. (D) Relative mRNA level of Ucp1, IL-6, Vegfa, Glut1, Glut4, Gatm, and Gamt ($n$ = 7–8), and (E) quantification of UCP1 protein level normalized to α-tubulin and Gapdh of BAT from mice repetitively exposed to PBS or HDM and fed with LFD or HFD ($n$ = 4). Mean ± SEM; one-way ANOVA with Tukey's multiple comparisons test. *$p < 0.05$; **$p < 0.01$; ***$p < 0.001$; ****$p < 0.0001$

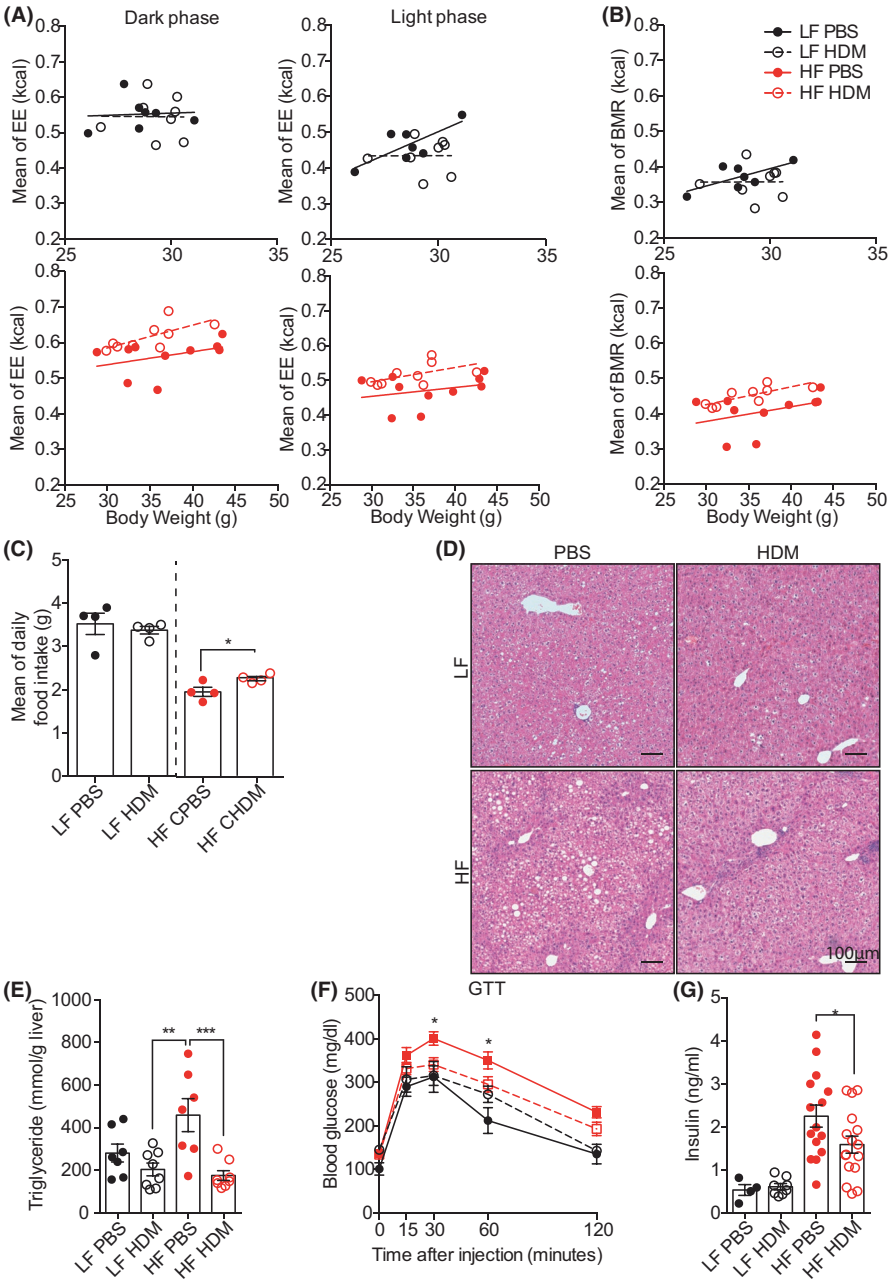


**FIGURE 5** Improvement of glucose tolerance and increase in energy expenditure in HFD-fed mice upon HDM exposure. (A) Indirect calorimetry performed at week 11–12. Mean energy expenditure (EE) correlated to body weight during dark phase (left panels) and light phase (right panels) of mice fed with LFD (upper panels) and HFD (lower panels) ($n$ = 4–8). (B) Mean basal metabolic rates (BMR) correlated to individual body weight of mice fed with LFD (upper panel) and HFD (lower panel) ($n$ = 4–8). (C) Mean daily food intake ($n$ = 4–8, each data point refers to mean food intake/day/mouse). (D) Representative image of H&E staining and (E) triglyceride content from liver samples of mice repetitively exposed to PBS or HDM and fed with LFD or HFD ($n$ = 7–8). (F) Glucose tolerance test after 9 weeks of diet ($n$ = 8–16) and (G) fasted serum insulin level collected after 10 weeks of diet ($n$ = 4–16) from mice repetitively exposed to PBS or HDM and fed with LFD or HFD diet ($n$ = 4–16). Mean ± SEM; one-way (Figure 5D,E,G) or two-way (Figure 5F) ANOVA with Tukey's multiple comparisons test. *$p < 0.05$; **$p < 0.01$; ***$p < 0.001$

(Figure 3D). Moreover, expression of the pro-inflammatory cytokine IL-17, inducing neutrophil recruitment and tissue inflammation,[35] was significantly reduced in HFD HDM mice compared to PBS controls (Figure 3D; $p$ = 0.0037). Thus, repetitive HDM exposure reduced the expression of pro-inflammatory cytokines and inflammatory cell infiltration in pgWAT, suggesting an overall positive impact on systemic metabolism.

### 3.4 | Increased browning in subcutaneous adipose tissue of HFD-fed HDM mice

In contrast to pgWAT, subcutaneous WAT (scWAT) is generally not associated with obesity-induced inflammation and accumulation of scWAT poorly associates with the development of the metabolic syndrome.[36] However, scWAT plays an important role

in regulation of systemic metabolism through the development of beige (brown-like) adipocytes, which in contrast to white fat, but similarly to brown fat, dissipate surplus energy in form of heat through mitochondrial uncoupling.[37] Similarly to pgWAT, scWAT mass was increased by HFD feeding, but did not differ between HDM and PBS (Figure S4, right). Furthermore, we could not observe morphological differences using H&E staining between groups (Figure 4A). Gene expression analysis confirmed the expected downregulation of the mitochondrial uncoupling protein UCP1 upon HFD feeding (Figure 4B).[38] We also observed a trend for reduced Ucp1 expression upon HDM exposure in LFD-fed mice, which was also observed for other beige adipocyte markers such as Cidea and Prdm16, but not Tmem26 and Ppargc1a. However, despite no difference in Ucp1 expression between groups upon HFD feeding, expression of the beige adipocyte markers Cidea, Prdm16, and Ppargc1a was significantly upregulated in HDM-treated HFD-fed mice, with a trend also observed in Tmem26 (Figure 4B). The increase of browning markers in scWAT was associated with an increased expression of IL-13 and IL-4 in HFD HDM mice compared to the other groups (Figure 4B).

The unexpected increase in expression of markers for thermogenic adipocytes led us to investigate brown adipose tissue (BAT) as the major site for thermogenesis through mitochondrial uncoupling. H&E staining of BAT showed increased lipid droplet size upon HFD feeding, but no apparent difference between PBS and HDM groups (Figure 4C). UCP1 mRNA and protein levels were not statistically different between control and HDM groups (Figure 4D,E), albeit a trend for reduced mRNA expression of Ucp1 (LFD $p = 0.7318$, HFD $p = 0.1664$) in HDM-exposed mice (Figure 4D). We also did not observe statistically significant differences in IL-6 (HFD $p = 0.1805$) or Glut4 (HFD $p = 0.7977$) expression (Figure 4D). However, expression of the vascular endothelial growth factor-a (Vegfa) ($p = <0.0001$) and Glut1 ($p = 0.0383$) was significantly increased in HFD-fed HDM-treated mice (Figure 4D). A similar increase was also observed for glycine amidinotransferase [Gatm; ($p = 0.0238$)] and guanidinoacetate N-methyltransferase [Gamt; ($p = 0.0139$)] (Figure 4D), two key enzymes in the creatine synthesis pathway,[39] an alternative UCP1 independent pathway for thermogenesis,[40] in HFD, but not in LFD-fed HDM mice compared to their respective PBS controls.

### 3.5 | Increased energy expenditure and improved glucose tolerance in HDM-exposed mice upon HFD feeding

These findings suggested a potential increase in thermogenesis and energy expenditure in HDM-exposed mice upon HFD feeding. To test a potential role of HDM exposure in the regulation of energy expenditure upon HFD feeding, we studied key metabolic parameters using indirect calorimetry. HDM-exposed HFD-fed mice showed increased energy expenditure in both the light and dark cycle (Figure 5A), whereas this was not observed in LFD-fed HDM mice. We did not observe differences in locomotor activity in HDM-exposed mice compared to their diet control (Figure S5A). However, consistent with the increased expression of markers of thermogenesis in scWAT and BAT, we observed an increased basal metabolic rate (BMR) (Figure 5B) in HFD-fed HDM mice. The increased energy expenditure, appeared to be offset by increased energy intake, as daily food intake was significantly increased (1.9 g/day ± 0.2 vs 2.3 g/day ± 0.2; $p = 0.0451$) in the HFD-fed HDM group compared to the diet control (Figure 5C), resulting in no net gain or loss of body weight and no changes in the respiratory quotient of HDM-exposed HFD-fed mice compared to the diet controls (Figure S5B).

Thus, prolonged HDM exposure reduced adipose tissue inflammation and increased thermogenic fat activity to increase energy expenditure upon HFD feeding, which are both associated with improved glucose and insulin metabolism and reduced hepatosteatosis. Histology (Figure 5D) and triglyceride measurements (Figure 5E) confirmed a reduction in hepatosteatosis in HDM-treated HFD-fed mice, with little differences observed in LFD diet mice.

To test the impact of the observed changes in adipose tissues and liver on glucose metabolism, we performed glucose and insulin tolerance tests at weeks 9 and 10, respectively, of the study. HDM exposure in LFD-fed mice had little effects on glucose and insulin tolerance (Figure 5F, Figure S5C). However, we observed an increase in fasting glycemia in HDM-exposed mice upon LFD feeding (Figure S5C). Conversely, glucose tolerance in HDM-exposed HFD-fed mice was improved (Figure 5F), with no differences in insulin tolerance (Figure S5C). Moreover, HDM exposure reduced random-fed insulin levels, albeit with great variability between individual mice (Figure 5G).

### 3.6 | HDM exposure induces small but significant changes in gut microbiota composition upon LFD and HFD feeding

Changes in the host metabolism can affect the structure and function of the gut microbiome and vice versa.[41-43] To this end, we analyzed gut microbial composition for HDM-treated LFD and HFD-fed mice as well as for the respective PBS controls. As previously shown, feeding a HFD had profound effects on the beta diversity of gut microbiota (Figure 6A). We did not observe statistically significant differences in beta diversity or at the level of individual families when comparing HDM to PBS mice irrespective of the diet (Figure 6A,B), suggesting that differences in diets have a dominant effect. However, when HDM-treated mice were compared to controls in their respective diet groups separately, we observed significant differences in beta diversity ($p = <0.001$ LFD and $p = <0.00201$ HFD) and at the level of individual families (Figure 6C,D). Interestingly, abundance of the family *Lactobacillaceae* was reduced in LFD-fed mice upon HDM treatment, which harbors a large number of bacteria with probiotic properties.[44] This could indicate that HDM-induced lung inflammation reduces the abundance of bacteria which promotes positive interactions with the host cells, similar to HFD feeding. In contrast to

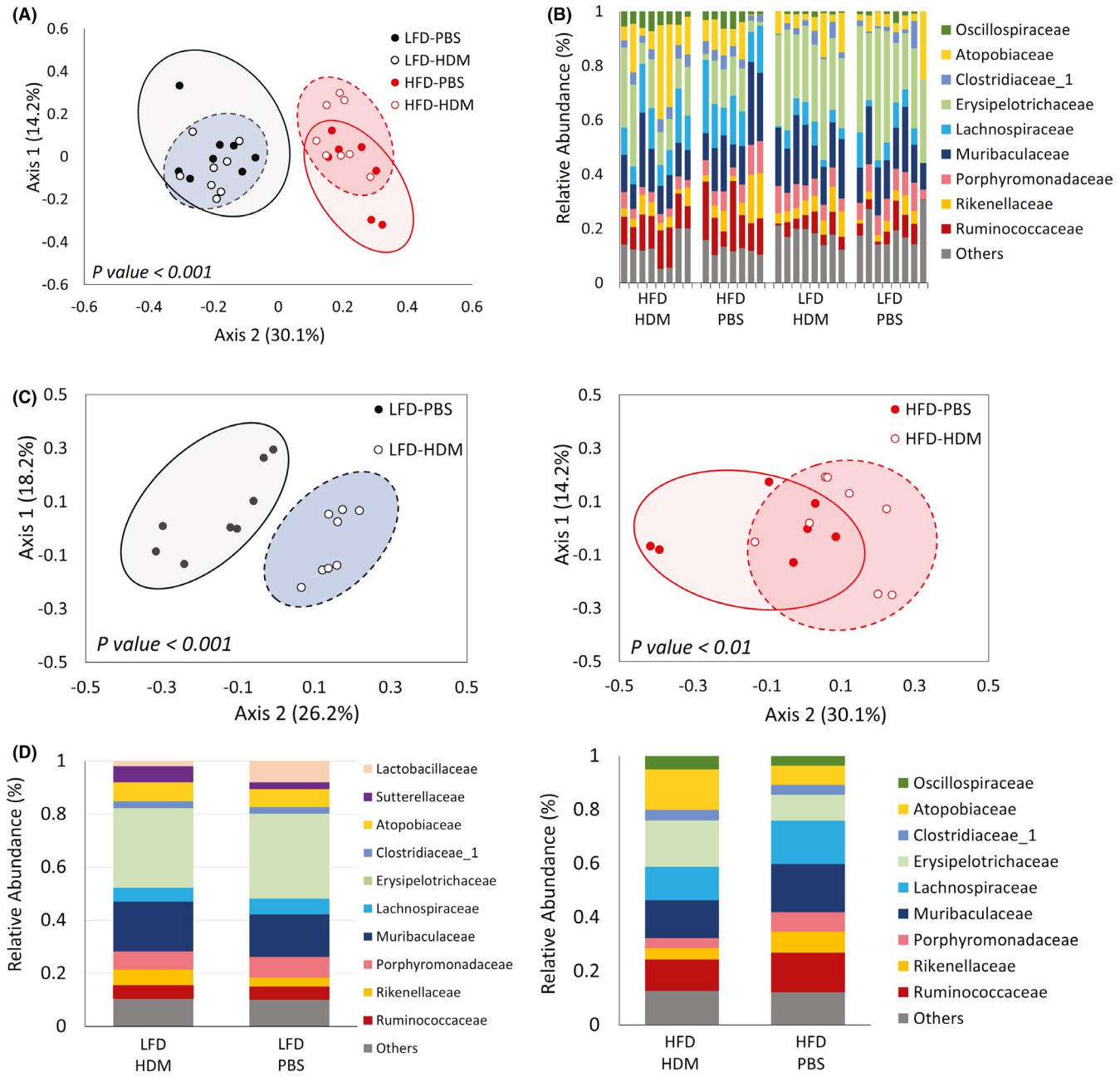


**FIGURE 6** Gut microbiota analysis of HDM-treated LFD and HFD mice. (A) Beta diversity analysis by PCoA and (B) taxonomy profiling at the family level for all treatment and diet groups. (C) Beta diversity analysis, for LFD and HFD-fed cohorts separately. (D) Top ten families for each diet group. Non-parametric Kruskal–Wallis test and Permanova for PCoA; $^{*}p < 0.05$; $^{**}p < 0.01$; and $^{***}p < 0.001$; $^{****}p < 0.0001$

*Lactobacillaceae*, *Sutterellaceae* strongly increased upon HDM exposure. *Sutterellaceae* have been detected previously as IgA degrading bacteria and associated with Ulcerative colitis.[45]

## 4 | DISCUSSION

The link between obesity and the metabolic syndrome is well established, however, increasing data also suggest an association between metabolic diseases and allergies.[46,47] In fact, adipokines and type 2 cytokines are now identified as main driver of immunosenescence.[48] Our analysis comprises data from 2207 adults from southern Germany and revealed no significant associations between body and fat mass with asthma or rhinitis. Conversely, we found a very strong direct association between WHR, which is a clinical parameter for body fat distribution and insulin resistance with asthma. However, various covariates, such as the environment, lifestyle, food choices, and the potentially long duration of disease development and progression pose a great epidemiological and clinical challenge for studying the mechanistic interactions of these diseases. Preclinical animal models provide a unique opportunity to control for most of the above-mentioned confounders, allowing to study the

mechanistic underpinnings of this association. We used prolonged exposure to the naturally occurring allergen HDM since it possesses higher clinical relevance compared to OVA and produces a strong immunological response in male C57BL/6 mice,[49] which are the primary rodent model for diet-induced obesity and insulin resistance.[50] Biweekly exposure to HDM maintained the tIgE response and lung pathology, characterized by mucus hypersecretion and infiltration of inflammatory cells until the end of the experiment, without promoting immunological tolerance, as previously suggested.[51] In fact, we observed increased GATA3$^+$, ST2$^+$, ROR$\gamma$t$^+$, in HDM allergic mice, whereas FoxP3$^+$ cells were increased to a lower degree.

However, parallel exposure to HFD did not exacerbate the inflammatory response. We show a dampened inflammatory infiltrate in the HFD-fed HDM group compared to the LFD HDM group. This is in contrast to a previous study observing increased allergic lung inflammation in HFD-fed mice.[52] A major difference in the experimental setup, however, may explain our diverging results. Everaere et al. applied the allergy protocol in obese and insulin-resistant mice, while we studied the co-development of both diseases, which may better reflect reality in most cases.[51] Conversely, our study is in line with data using an OVA/alum sensitization model, which also showed reduced lung inflammation upon HFD feeding.[53] Notably, this study used female mice, which are protected from diet-induced obesity and insulin resistance, suggesting that the observed reduction in lung inflammation is a direct consequence of the diet rather excessive fat mass and insulin resistance.

Prolonged HDM exposure reduced neutrophil and Th17 cell numbers in pgWAT and expression of macrophage markers and pro-inflammatory cytokines as IL-6, IL-1$\beta$ and IL-17a especially upon HFD feeding. Obesity-associated adipose tissue inflammation is a key element in the initiation of local and systemic insulin resistance.[54-57]

In line with a protective effect of reduced adipose inflammation on the liver and systemic glucose metabolism, we observed a reduction in hepatic triglyceride levels and improved glucose tolerance in HDM-exposed HFD-fed mice. In parallel to the reduced pgWAT inflammation, we also observed an increased basal metabolic rate and energy expenditure, which correlated with increased expression of thermogenic markers in scWAT and BAT. Expression of Cidea, Prdm16, Tmem26, and Ppargc1a, all markers for brown and beige adipocytes, was increased in scWAT of HDM-exposed HFD-fed mice.[58,59] A potential link between HDM-induced inflammation and increased thermogenic gene expression in scWAT is via the observed increase in IL-13 and IL-4 expression. This could activate eosinophils to secrete IL-4, which acts directly on Pdgfra$^+$ precursor cells to increase the proliferation and differentiation of beige/ thermogenic adipocytes.[59] In addition to beige adipocytes, BAT contributes significantly to thermogenesis and previous studies suggested an AMPK/Ppargc1a pathway to drive thermogenic gene expression in BAT of ovalbumin-induced asthmatic mice.[12] However, we did not observe increased Ucp1 mRNA or protein levels in the HFD HDM group. Instead, we observed increased expression of key components of the creatinine cycle, a recently identified alternative thermogenic pathway.[39,60] The link between these changes in BAT and HDM-induced lung inflammation in context of HFD feeding will require additional studies to identify key proteins mediating these effects.

Nevertheless, our animal data are in contradiction to the epidemiological associations observed in our study cohort that showed a negative effect of asthma on glucose homeostasis. However, we conclude that the positive metabolic effects of repeated HDM exposure in mice are not observed in humans, as the contribution of thermogenic fat to energy turnover is much lower in humans than in mice. Moreover, our epidemiological data have studied adults where asthma could have been already established and we did not specifically study HDM-induced allergies but asthma in general, which could include several different, in part seasonal allergies. Here, doctor-diagnosed asthma was requested via questionnaire and self-reported by the study participants. In addition, information on symptoms and asthma medication was available but not on allergic vs. non-allergic asthma or asthma severity. Furthermore, the study population was on average 60 years of age and thus older than most cohort studies focused on allergic diseases. However, the high prevalence of metabolic diseases in this age group and the comprehensive assessment of metrics of body fat content and insulin sensitivity enables research on the long-term interactions of asthma and metabolic disease. To this end, it would be very interesting to obtain data to correlate human BAT activity with the metabolic consequences of HDM allergies. We provide for the first time experimental data on the co-development of HDM-induced allergic lung inflammation and diet-induced obesity. Unlike previous studies, our focus was on the co-occurrence of both incidences, considering this a situation closer to the patients' reality. Interestingly, our experimental setup, with prolonged HDM exposure and HFD feeding in obesity-prone mice revealed that chronic HDM-induced inflammation has beneficial consequences on the inflammatory and functional status of key metabolic organs such as adipose tissue and the liver to ameliorate the effects of diet-induced obesity. We expect that our data will inform future epidemiological and clinical studies aiming to dissociate the co-occurrence of metabolic and allergic pathologies, potentially using changes in gut microbiota as biomarkers, and thereby improve quality of life for a large number of patients.

## ACKNOWLEDGEMENTS

The authors wish to thank the animal caretakers of the Helmholtz Center Munich and Johanna Grosch and Benjamin Schnautz for technical assistance. The authors express appreciation to all attendees for their active participation in the KORA study and thank the field staff in Augsburg conducting the KORA study. Open access funding enabled and organized by ProjektDEAL.

## CONFLICT OF INTEREST

The authors declare no conflict of interest.

## AUTHOR CONTRIBUTIONS

RK, CBS, CTH, FA, and SU designed the experiments. RK, SM, ES, IA, and FA performed experiments. CF, JN, AP, HS, and MSta analyzed

epidemiological data. RK, FA, and SU wrote the manuscript. RK and SM performed data analysis. MB, AUN, SG, and MSch analyzed microbial data. All authors participated in editing the manuscript.

## DATA AVAILABILITY STATEMENT

The data from the KORA study are subject to national data protection laws and restrictions were imposed by the Ethics Committee of the Bavarian Chamber of Physicians to ensure data privacy of the study participants. Therefore, data cannot be made freely available in a public repository. Applications for access to the data sets can be found at the following link: https://www.helmholtz-muenchen.de/en/kora/for-scientists/cooperation-with-kora/index.html. Data can be requested through an individual project agreement with KORA via the online portal KORA.PASST (https://epi.helmholtz-muenchen.de) and requests are subject to approval by the KORA Board.

## ORCID

*Madhumita Bhattacharyya* https://orcid.org/0000-0002-7671-6967
*Carsten B. Schmidt-Weber* https://orcid.org/0000-0002-3203-8084
*Marie Standl* https://orcid.org/0000-0002-5345-2049
*Francesca Alessandrini* https://orcid.org/0000-0002-9854-8968
*Siegfried Ussar* https://orcid.org/0000-0001-7575-0920

## REFERENCES

1. Wells JC, Siervo M. Obesity and energy balance: is the tail wagging the dog? *Eur J Clin Nutr*. 2011;65(11):1173-1189.
2. Huang PL. A comprehensive definition for metabolic syndrome. *Dis Model Mech*. 2009;2(5-6):231-237.
3. Saklayen MG. The global epidemic of the metabolic syndrome. *Curr Hypertens Rep*. 2018;20(2):12.
4. Chalk MB. Obesity: addressing a multifactorial disease. *Case Manager*. 2004;15(6):47-49. quiz 50.
5. Traidl-Hoffmann C. Allergie – eine Umwelterkrankung! *Bundesgesundheitsblatt Gesundheitsforschung Gesundheitsschutz*. 2017;60(6):584-591.
6. Burbank AJ, Sood AK, Kesic MJ, Peden DB, Hernandez ML. Environmental determinants of allergy and asthma in early life. *J Allergy Clin Immunol*. 2017;140(1):1-12.
7. Kanchongkittiphon W, Mendell MJ, Gaffin JM, Wang G, Phipatanakul W. Indoor environmental exposures and exacerbation of asthma: an update to the 2000 review by the Institute of Medicine. *Environ Health Perspect*. 2015;123(1):6-20.
8. Peters U, Dixon AE, Forno E. Obesity and asthma. *J Allergy Clin Immunol*. 2018;141(4):1169-1179.
9. Park S, Choi N-K, Kim S, Lee C-H. The relationship between metabolic syndrome and asthma in the elderly. *Sci Rep*. 2018;8(1):9378.
10. Hersoug LG, Linneberg A. The link between the epidemics of obesity and allergic diseases: does obesity induce decreased immune tolerance? *Allergy*. 2007;62(10):1205-1213.
11. De Rosa V, Procaccini C, Cali G, et al. A key role of leptin in the control of regulatory T cell proliferation. *Immunity*. 2007;26(2):241-255.
12. Song X, Li B, Wang H, et al. Asthma alleviates obesity in males through regulating metabolism and energy expenditure. *Biochim Biophys Acta Mol Basis Dis*. 2019;1865(2):350-359.
13. Schoettl T, Fischer IP, Ussar S. Heterogeneity of adipose tissue in development and metabolic function. *J Exp Biol*. 2018;221(Suppl 1):jeb162958.
14. Fassio F, Guagnini F. House dust mite-related respiratory allergies and probiotics: a narrative review. *Clin Mol Allergy*. 2018;16(1):15.
15. Holle R, Happich M, Löwel H, Wichmann H, Group MKS. KORA – a research platform for population based health research. *Gesundheitswesen*. 2005;67(Suppl 1):S19-S25.
16. Luzak A, Karrasch S, Thorand B, et al. Association of physical activity with lung function in lung-healthy German adults: results from the KORA FF4 study. *BMC Pulm Med*. 2017;17(1):215.
17. Qiao Q, Nyamdorj R. The optimal cutoff values and their performance of waist circumference and waist-to-hip ratio for diagnosing type II diabetes. *Eur J Clin Nutr*. 2010;64(1):23-29.
18. Markus MRP, Rospleszcz S, Ittermann T, et al. Glucose and insulin levels are associated with arterial stiffness and concentric remodeling of the heart. *Cardiovasc Diabetol*. 2019;18(1):145.
19. Kyle UG, Genton L, Karsegard L, Slosman DO, Pichard C. Single prediction equation for bioelectrical impedance analysis in adults aged 20–94 years. *Nutrition*. 2001;17(3):248-253.
20. Huemer MT, Huth C, Schederecker F, et al. Association of endothelial dysfunction with incident prediabetes, type 2 diabetes and related traits: the KORA F4/FF4 study. *BMJ Open Diabetes Res Care*. 2020;8(1):e001321.
21. Sujana C, Seissler J, Jordan J, et al. Associations of cardiac stress biomarkers with incident type 2 diabetes and changes in glucose metabolism: KORA F4/FF4 study. *Cardiovasc Diabetol*. 2020;19(1):178.
22. Vardeny O, Gupta DK, Claggett B, et al. Insulin resistance and incident heart failure the ARIC study (atherosclerosis risk in communities). *JACC Heart Fail*. 2013;1(6):531-536.
23. Rathmann W, Kowall B, Tamayo T, et al. Hemoglobin A1c and glucose criteria identify different subjects as having type 2 diabetes in middle-aged and older populations: the KORA S4/F4 Study. *Ann Med*. 2012;44(2):170-177.
24. Alessandrini F, Schulz H, Takenaka S, et al. Effects of ultrafine carbon particle inhalation on allergic inflammation of the lung. *J Allergy Clin Immunol*. 2006;117(4):824-830.
25. Lueders T, Manefield M, Friedrich MW. Enhanced sensitivity of DNA- and rRNA-based stable isotope probing by fractionation and quantitative analysis of isopycnic centrifugation gradients. *Environ Microbiol*. 2004;6(1):73-78.
26. Klindworth A, Pruesse E, Schweer T, et al. Evaluation of general 16S ribosomal RNA gene PCR primers for classical and next-generation sequencing-based diversity studies. *Nucleic Acids Res*. 2013;41(1):e1.
27. Alessandrini F, Vennemann A, Gschwendtner S, et al. Pro-inflammatory versus immunomodulatory effects of silver nanoparticles in the lung: the critical role of dose, size and surface modification. *Nanomaterials (Basel)*. 2017;7(10):300.
28. Callahan BJ, McMurdie PJ, Rosen MJ, Han AW, Johnson AJ, Holmes SP. DADA2: high-resolution sample inference from Illumina amplicon data. *Nat Methods*. 2016;13(7):581-583.
29. Yoon SH, Ha SM, Kwon S, et al. Introducing EzBioCloud: a taxonomically united database of 16S rRNA gene sequences and whole-genome assemblies. *Int J Syst Evol Microbiol*. 2017;67(5):1613-1617.
30. Federhen S. The NCBI taxonomy database. *Nucleic Acids Res*. 2012;40(Database issue):D136-D143.
31. Cole JR, Wang Q, Cardenas E, et al. The ribosomal database Project: improved alignments and new tools for rRNA analysis. *Nucleic Acids Res*. 2009;37(Database issue):D141-D145.
32. Quast C, Pruesse E, Yilmaz P, et al. The SILVA ribosomal RNA gene database project: improved data processing and web-based tools. *Nucleic Acids Res*. 2013;41(Database issue):D590-D596.
33. Chong J, Liu P, Zhou G, Xia J. Using MicrobiomeAnalyst for comprehensive statistical, functional, and meta-analysis of microbiome data. *Nat Protoc*. 2020;15(3):799-821.
34. Lumeng CN, Bodzin JL, Saltiel AR. Obesity induces a phenotypic switch in adipose tissue macrophage polarization. *J Clin Invest*. 2007;117(1):175-184.

35. Ahmed M, Gaffen SL. IL-17 in obesity and adipogenesis. *Cytokine Growth Factor Rev*. 2010;21(6):449-453.
36. Poret JM, Souza-Smith F, Marcell SJ, et al. High fat diet consumption differentially affects adipose tissue inflammation and adipocyte size in obesity-prone and obesity-resistant rats. *Int J Obes (Lond)*. 2018;42(3):535-541.
37. Harms M, Seale P. Brown and beige fat: development, function and therapeutic potential. *Nat Med*. 2013;19(10):1252-1263.
38. Cannon B, Nedergaard J. Brown adipose tissue: function and physiological significance. *Physiol Rev*. 2004;84(1):277-359.
39. Kazak L, Cohen P. Creatine metabolism: energy homeostasis, immunity and cancer biology. *Nat Rev Endocrinol*. 2020;16(8):421-436.
40. Kazak L, Chouchani ET, Lu GZ, et al. Genetic depletion of adipocyte creatine metabolism inhibits diet-induced thermogenesis and drives obesity. *Cell Metab*. 2017;26(4):660-671.e663.
41. Ussar S, Griffin NW, Bezy O, et al. Interactions between gut microbiota, host genetics and diet modulate the predisposition to obesity and metabolic syndrome. *Cell Metab*. 2015;22(3):516-530.
42. Ussar S, Fujisaka S, Kahn CR. Interactions between host genetics and gut microbiome in diabetes and metabolic syndrome. *Mol Metab*. 2016;5(9):795-803.
43. Fujisaka S, Ussar S, Clish C, et al. Antibiotic effects on gut microbiota and metabolism are host dependent. *J Clin Invest*. 2016;126(12):4430-4443.
44. Behnsen J, Deriu E, Sassone-Corsi M, Raffatellu M. Probiotics: properties, examples, and specific applications. *Cold Spring Harb Perspect Med*. 2013;3(3):a010074.
45. Kaakoush NO. Sutterella species, IgA-degrading bacteria in ulcerative colitis. *Trends Microbiol*. 2020;28(7):519-522.
46. Lugogo NL, Hollingsworth JW, Howell DL, et al. Alveolar macrophages from overweight/obese subjects with asthma demonstrate a proinflammatory phenotype. *Am J Respir Crit Care Med*. 2012;186(5):404-411.
47. Serafino-Agrusa L. Asthma and metabolic syndrome: Current knowledge and future perspectives. *World J Clin Cases*. 2015;3(3):285.
48. Sayed N, Huang Y, Nguyen K, et al. An inflammatory aging clock (iAge) based on deep learning tracks multimorbidity, immunosenescence, frailty and cardiovascular aging. *Nature Aging*. 2021;1(7):598-615.
49. Alessandrini F, Musiol S, Schneider E, Blanco-Perez F, Albrecht M. Mimicking antigen-driven asthma in rodent models-how close can we get? *Front Immunol*. 2020;11:575936.
50. Avtanski D, Pavlov VA, Tracey KJ, Poretsky L. Characterization of inflammation and insulin resistance in high-fat diet-induced male C57BL/6J mouse model of obesity. *Animal Model Exp Med*. 2019;2(4):252-258.
51. Bracken SJ, Adami AJ, Szczepanek SM, et al. Long-term exposure to house dust mite leads to the suppression of allergic airway disease despite persistent lung inflammation. *Int Arch Allergy Immunol*. 2015;166(4):243-258.
52. Everaere L, Ait-Yahia S, Molendi-Coste O, et al. Innate lymphoid cells contribute to allergic airway disease exacerbation by obesity. *J Allergy Clin Immunol*. 2016;138(5):1309-1318.e1311.
53. Schröder T, Wiese AV, Ender F, et al. Short-term high-fat diet feeding protects from the development of experimental allergic asthma in mice. *Clin Exp Allergy*. 2019;49(9):1245-1257.
54. Hotamisligil GS, Murray DL, Choy LN, Spiegelman BM. Tumor necrosis factor alpha inhibits signaling from the insulin receptor. *Proc Natl Acad Sci*. 1994;91(11):4854-4858.
55. Hoene M, Weigert C. The role of interleukin-6 in insulin resistance, body fat distribution and energy balance. *Obes Rev*. 2007;9(1):20-29.
56. Bril F, Barb D, Portillo-Sanchez P, et al. Metabolic and histological implications of intrahepatic triglyceride content in nonalcoholic fatty liver disease. *Hepatology*. 2017;65(4):1132-1144.
57. Bevilacqua S, Bonadonna R, Buzzigoli G, et al. Acute elevation of free fatty acid levels leads to hepatic insulin resistance in obese subjects. *Metabolism*. 1987;36(5):502-506.
58. Karlina R, Lutter D, Miok V, et al. Identification and characterization of distinct brown adipocyte subtypes in C57BL/6J mice. *Life Sci Alliance*. 2020;4(1):e202000924.
59. Wang W, Seale P. Control of brown and beige fat development. *Nat Rev Mol Cell Biol*. 2016;17(11):691-702.
60. Kazak L, Rahbani JF, Samborska B, et al. Ablation of adipocyte creatine transport impairs thermogenesis and causes diet-induced obesity. *Nat Metab*. 2019;1(3):360-370.

## SUPPORTING INFORMATION

Additional supporting information may be found in the online version of the article at the publisher's website.

**How to cite this article:** Karlina R, Flexeder C, Musiol S, et al. Differential effects of lung inflammation on insulin resistance in humans and mice. *Allergy*. 2022;00:1–16. doi:10.1111/all.15226

# Supplementary Figure 1

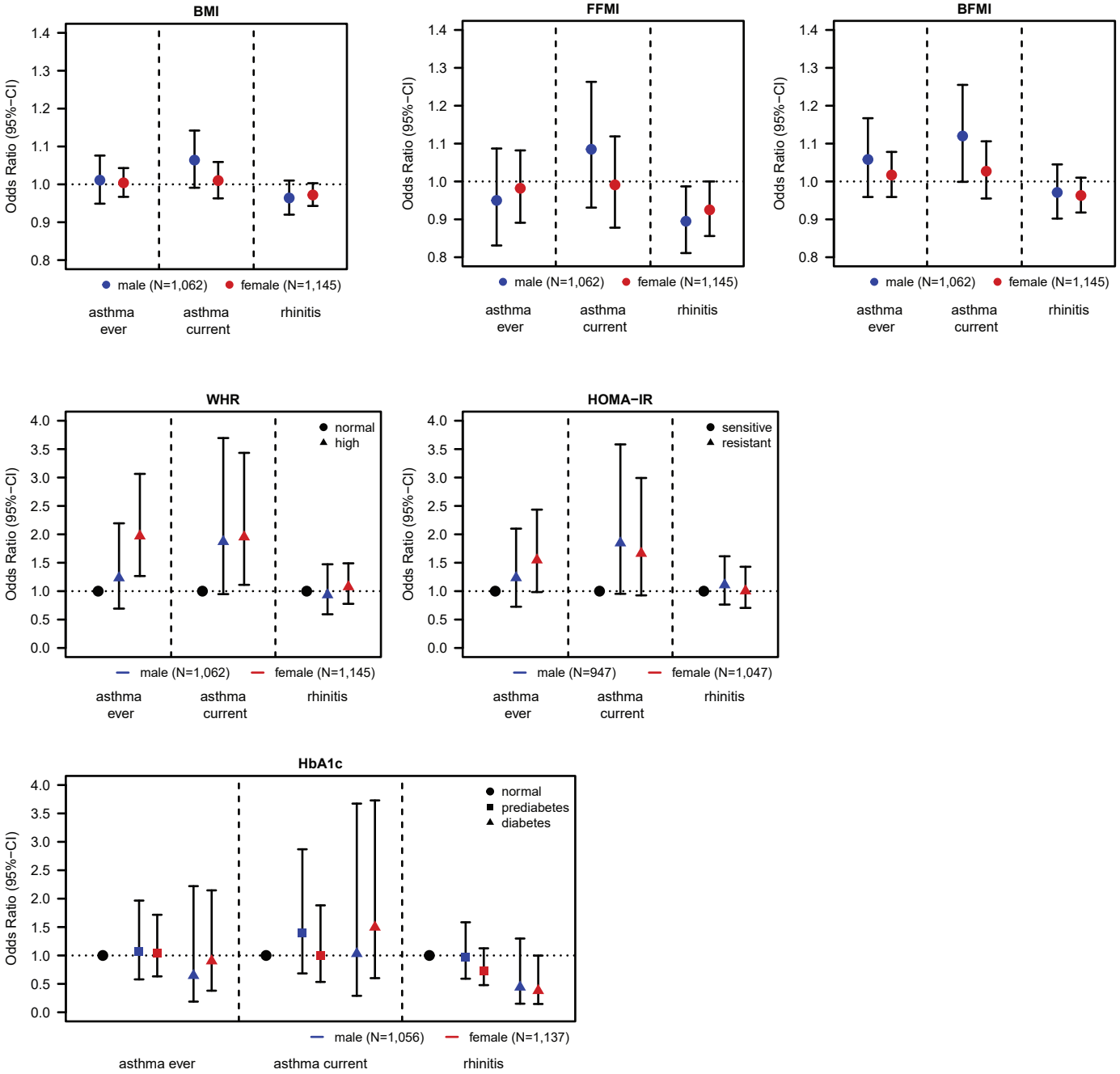

**Supplementary Figure 2**

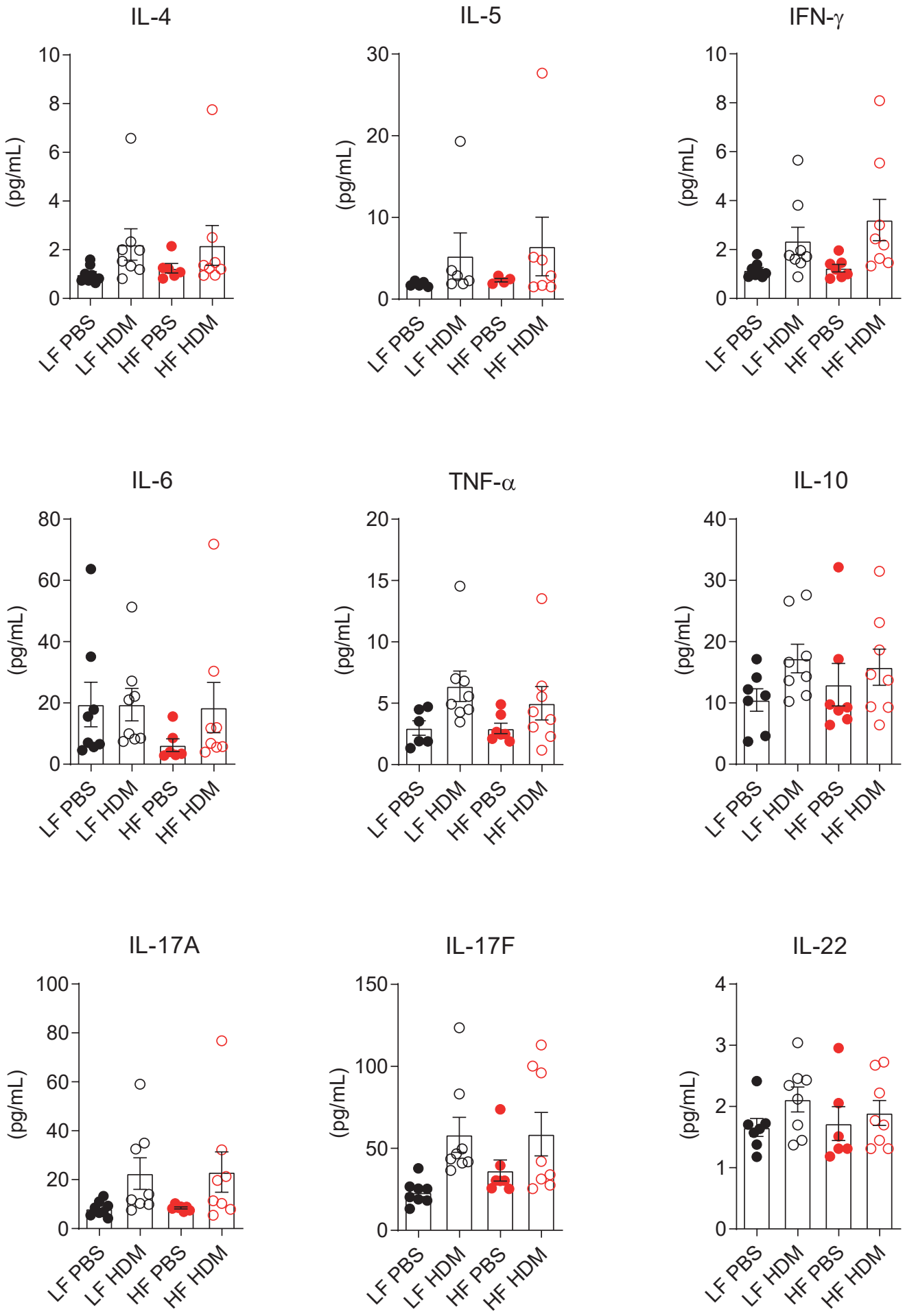

## Supplementary Figure 3

(A)

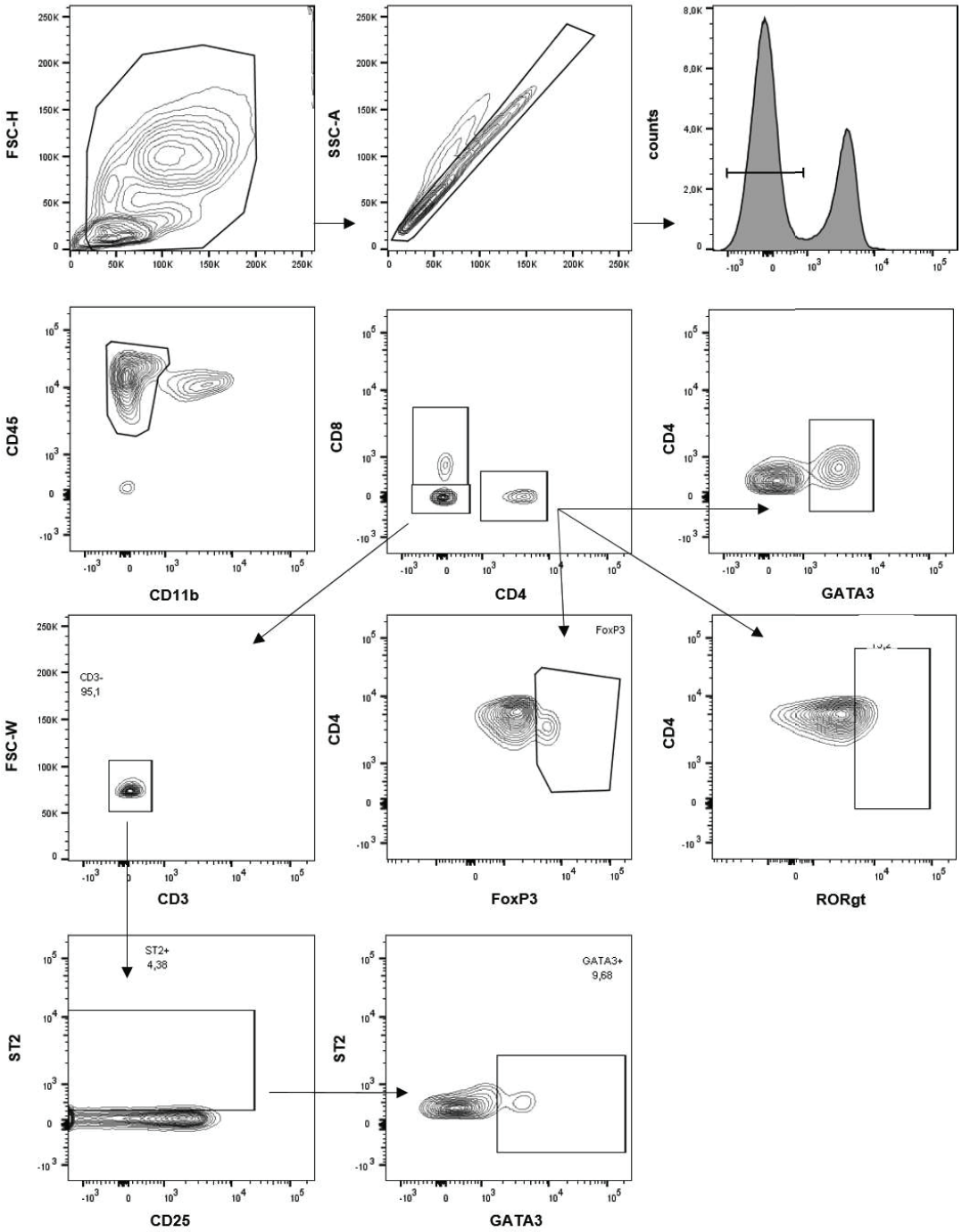


(B)

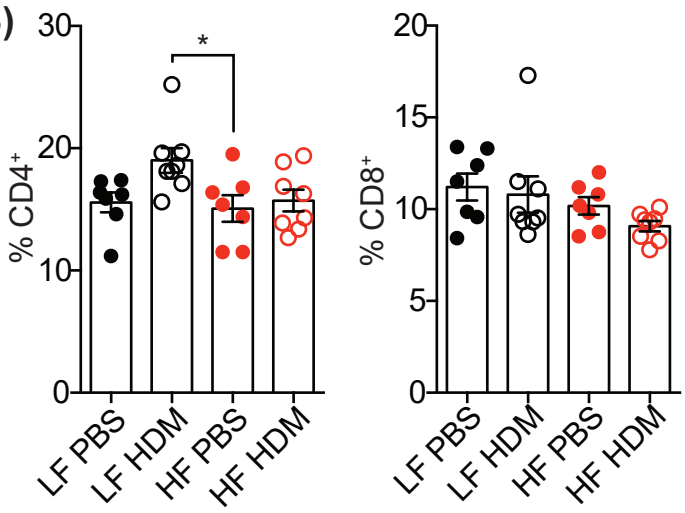

## Supplementary Figure 4

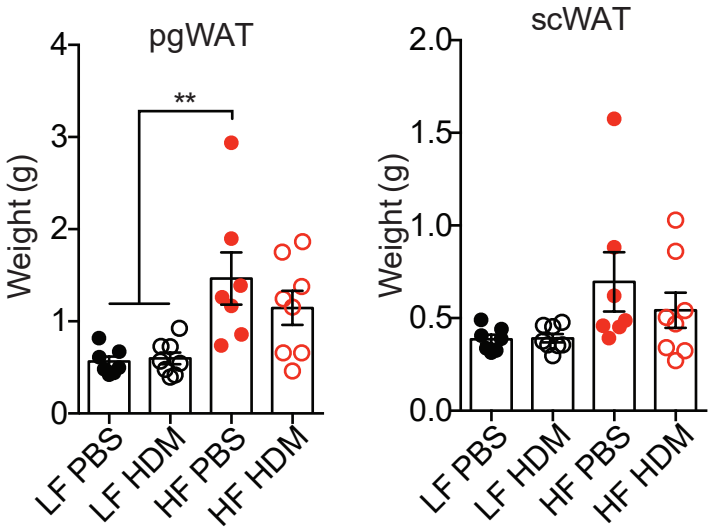

**Supplementary Figure 5**

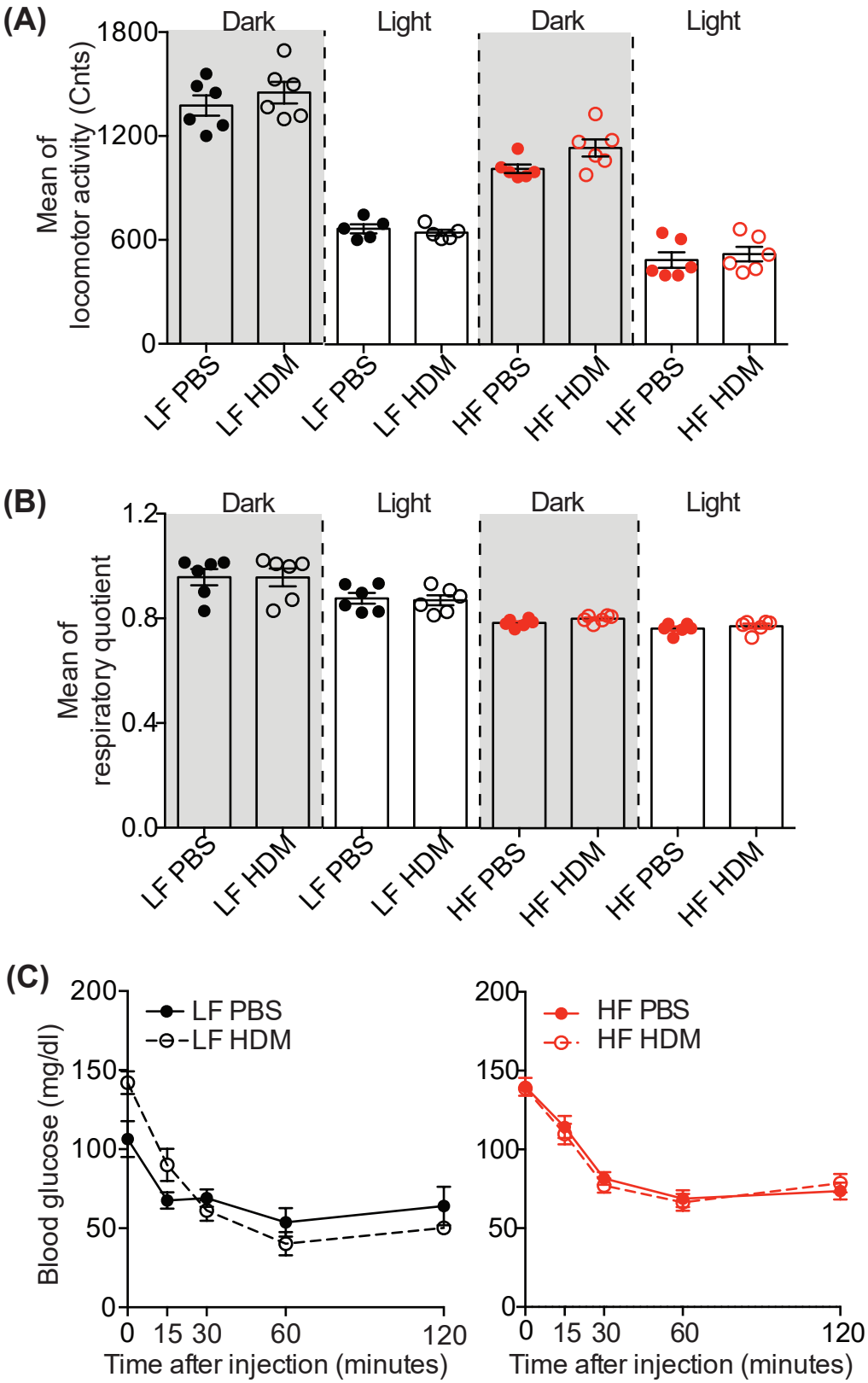

## Supplementary Tables

### Table S1: Descriptive characteristics of the study population

| | mean (SD) or % (n/N) | | | |
|---|---|---|---|---|
| | **total (n=2207)** | **male (n=1062)** | **female (n=1145)** | **p-value** |
| Age, years | 60.0 (12.2) | 60.4 (12.4) | 59.6 (12.0) | 0.106 |
| Sex | | | | |
| male | 48.1 (1062/2207) | 100.0 (1062/1062) | 0.0 (0/1145) | |
| female | 51.9 (1145/2207) | 0.0 (0/1062) | 100.0 (1145/1145) | |
| Education | | | | |
| low | 48.4 (1069/2207) | 49.4 (525/1062) | 47.5 (544/1145) | |
| medium | 25.9 (571/2207) | 20.0 (212/1062) | 31.4 (359/1145) | |
| high | 25.7 (567/2207) | 30.6 (325/1062) | 21.1 (242/1145) | <0.001 |
| Alcohol intake | | | | |
| no | 26.8 (592/2207) | 17.9 (190/1062) | 35.1 (402/1145) | |
| low | 54.6 (1204/2207) | 60.9 (647/1062) | 48.6 (557/1145) | |
| moderate | 18.6 (411/2207) | 21.2 (225/1062) | 16.2 (186/1145) | <0.001 |
| Physical activity | | | | |
| high | 25.9 (572/2207) | 28.3 (301/1062) | 23.7 (271/1145) | |
| moderate | 31.4 (693/2207) | 27.5 (292/1062) | 35.0 (401/1145) | |
| low | 14.7 (324/2207) | 14.3 (152/1062) | 15.0 (172/1145) | |
| no | 28.0 (618/2207) | 29.8 (317/1062) | 26.3 (301/1145) | 0.001 |
| Smoking status | | | | |
| current | 15.5 (343/2207) | 16.8 (178/1062) | 14.4 (165/1145) | |
| former | 42.6 (941/2207) | 50.2 (533/1062) | 35.6 (408/1145) | |
| never | 41.8 (923/2207) | 33.1 (351/1062) | 50.0 (572/1145) | <0.001 |
| Diabetes mellitus | | | | |
| no | 90.2 (1984/2200) | 88.0 (934/1061) | 92.2 (1050/1139) | |
| type 2 | 9.8 (216/2200) | 12.0 (127/1061) | 7.8 (89/1139) | 0.001 |
| Hypertension, % | 38.6 (853/2207) | 43.4 (461/1062) | 34.2 (392/1145) | <0.001 |
| BMI, kg/m² | 27.7 (4.8) | 28.1 (4.1) | 27.4 (5.4) | <0.001 |
| BMI categories | | | | |
| <25 kg/m² | 30.9 (682/2207) | 22.9 (243/1062) | 38.3 (439/1145) | |
| >=25 - <30 kg/m² | 41.5 (915/2207) | 48.6 (516/1062) | 34.8 (399/1145) | |
| >=30 - <35 kg/m² | 19.7 (434/2207) | 22.6 (240/1062) | 16.9 (194/1145) | |
| >= 35 kg/m² | 8.0 (176/2207) | 5.9 (63/1062) | 9.9 (113/1145) | <0.001 |
| BFMI, kg/m² | 9.3 (3.3) | 8.0 (2.5) | 10.5 (3.5) | <0.001 |
| FFMI, kg/m² | 18.4 (2.6) | 20.1 (1.9) | 16.9 (2.1) | <0.001 |
| WHR | 0.9 (0.1) | 1.0 (0.1) | 0.8 (0.1) | <0.001 |

| | | | | |
|---|---|---|---|---|
| WHR categories | | | | |
| normal | 59.9 (1323/2207) | 70.5 (749/1062) | 50.1 (574/1145) | |
| high | 40.1 (884/2207) | 29.5 (313/1062) | 49.9 (571/1145) | <0.001 |
| HOMA-IR* | 2.2 (1.9) | 2.4 (1.9) | 2.0 (1.9) | <0.001 |
| HOMA-IR categories | | | | |
| insulin sensitive | 60.1 (1199/1994) | 54.6 (517/947) | 65.1 (682/1047) | |
| insulin resistant | 39.9 (795/1994) | 45.4 (430/947) | 34.9 (365/1047) | <0.001 |
| HbA1c, % | 5.5 (0.6) | 5.6 (0.7) | 5.5 (0.6) | 0.255 |
| HbA1c categories | | | | |
| normal | 72.6 (1593/2193) | 71.9 (759/1056) | 73.4 (834/1137) | |
| prediabetes | 21.5 (471/2193) | 21.8 (230/1056) | 21.2 (241/1137) | |
| diabetes | 5.9 (129/2193) | 6.3 (67/1056) | 5.5 (62/1137) | 0.609 |
| Rhinitis (DD), % | 18.6 (411/2207) | 17.3 (184/1062) | 19.8 (227/1145) | 0.146 |
| Asthma ever (DD), % | 8.6 (190/2207) | 7.2 (76/1062) | 10.0 (114/1145) | 0.023 |
| Asthma current, % | 5.3 (118/2207) | 4.6 (49/1062) | 6.0 (69/1145) | 0.168 |
| Wheezing, % | 9.0 (198/2207) | 8.9 (95/1062) | 9.0 (103/1145) | 1.000 |
| Asthma medication, % | 4.8 (107/2207) | 4.3 (46/1062) | 5.3 (61/1145) | 0.322 |

Study characteristics are described using mean and SD or percentages and frequencies (%, n/N). Differences between males and females were tested using Pearson's Chi-squared test for categorical variables and t-test for continuous variables. Current asthma is defined fulfilling at least two out of the following three criteria: ever doctor-diagnosed asthma, wheezing within the last 12 months and current asthma medication. Abbreviations: BMI, body mass index; BFMI, body fat mass index; FFMI, fat free mass index; WHR, waist to hip ratio; HOMA-IR, homeostasis model assessment-estimated insulin resistance; HbA1c, hemoglobin A1c; DD, doctor-diagnosed; SD, standard deviation. * = reported as geometric mean and SD

## Table S4: List of antibodies for FACS analysis

| Antibody | Clone | Company |
|---|---|---|
| CD3 | 17A2 | BioLegend |
| CD4 | L3T4 | BioLegend |
| CD45 | 30-F11 | BD |
| CD8 | 53-6.7 | eBioScience |
| CD11b | M1/70 | BioLegend |
| CD25 | PC61 | BioLegend |
| ST2 | DIH9 | BioLegend |
| FoxP3 | FJK-16s | eBioScience |
| GATA3 | TWAJ | eBioScience |
| RORc | AFKJS-9 | eBioScience |
| Zombie Aqua™ Fixable Viability Kit | | BioLegend |

## Table S5: List of qPCR primers 5' – 3'

| Gene | Forward sequence | Reverse sequence |
|---|---|---|
| *Cd68* | TCACCTTGACCTGCTCTCTC | AGGCCAATGATGAGAGGCAG |
| *Cidea* | CGGGAATAGCCAGAGTCACC | TGTGCATCGGATGTCGTAGG |
| *Gamt* | GCAGCCACATAAGGTTGTTCC | CTCTTCAGACAGCGGGTACG |
| *Gatm* | GACCTGGTCTTGTGCTCTCC | GGGATGACTGGTGTTGGAGG |
| *Glut1* | AACTGGGCAAGTCCTTTG | TTCTTCTCCCGCATCATCTG |
| *Glut4* | TGATTCTGCTGCCCTTCTGT | GGACATTGGACGCTCTCTCT |
| *Ifnγ* | GCCAGTTCCTCCAGATATCCA | CCACGGCACAGTCATTGAAA |
| *IL-1β* | CTGAAAGCTCTCCACCTCAA | CCCAAGGCCACAGGTATTTT |
| *IL-4* | TCAGTGATGTGGACTTGGAC | GAGCTGCAGAGACTCTTTCG |
| *IL-6* | GTCGGAGGCTTAATTACACATGT | CAAGTGCATCATCGTTGTTCA |
| *IL-10* | GGCCTTGTAGACACCTTGGT | CTCCCCTGTGAAAATAAGAGCA |
| *IL-13* | TGGTATGGAGTGTGGACCTG | CTGGGTCCTGTAGATGGCAT |
| *IL-17A* | GCCAGGAGTATGAAGTGACTG | CACAGTCAGGCACAAAGATGA |
| *Ppargc1α* | AGCCGTGACCACTGACAACGAG | GCTGCATGGTTCTGAGTGCTAAG |
| *Prdm16* | CCCACCAGACTTCGAGCTAC | ATCTCCCATCCAAAGTCGGC |
| *Tbp* | ACCCTTCACCAATGACTCCTATG | TGACTGCAGCAAATCGCTTGG |
| *Tmem26* | GAAACCAGTATTGCAGCACCC | CCCATTCCATTGGTGGCTCT |
| *Tnfα* | CCCACGTCGTAGCAAACCA | GTCTTTGAGATCCATGCCGTTG |
| *Ucp1* | CTGCCAGGACAGTACCCAAG | TCAGCTGTTCAAAGCACACA |

| *Vegfa* | CCACGACAGAAGGAGAGCAG | GTCCACCAGGGTCTCAATCG |
|---|---|---|

## Supplementary Figure Legends

**Supplementary Figure1: Epidemiological association between asthma and rhinitis with metrics of body fat content and insulin sensitivity, stratified by sex**

Logistic regression models were calculated separately for males and females and adjusted for age, smoking status, education level, physical activity, alcohol consumption and hypertension. Current asthma is defined as fulfilling at least two out of the following three criteria: ever doctor-diagnosed asthma, wheezing within the last 12 months and current asthma medication. WHR is defined as normal vs. high with cut-off >=1 for males and >=0.85 for females. HOMA-IR is categorized into insulin sensitive (HOMA-IR <2.5) and insulin resistant (HOMA-IR >=2.5) whereas HbA1c is categorized into normal (<5.7%), prediabetes (>=5.7% and <6.5%) and diabetes (>=6.5%). Results are presented as odds ratios (OR) with corresponding 95% confidence interval (CI).

**SUPPLEMENTARY FIGURE 2:** Cytokine analysis of BAL fluid from mice repetitively exposed to PBS or HDM and fed with LFD or HFD measured at the end (week 12) of experiment (n= 7-8).

**SUPPLEMENTARY FIGURE 3:** (A) Gating strategy employed for FACS analysis of lung tissue. (B) FACS analysis of lungs measuring the percentage of $CD4^+$ and $CD8^+$ of $CD45^+CD11b^-$ cells from mice constantly exposed to PBS or HDM and fed with LFD or HFD (n= 7-8).

**SUPPLEMENTARY FIGURE 4:** The weight of pgWAT and scWAT from mice constantly exposed to PBS or HDM and fed with LFD or HFD (n= 7-8).

**SUPPLEMENTARY FIGURE 5:** Indirect calorimetry of mice constantly exposed to PBS or HDM and fed with LFD and HFD at week 11 (dark phase is shown in grey shade). (A)

Mean respiratory quotient (n= 4-8) and (B) mean locomotor activity (n= 4-8) for light or dark cycle. (C) Insulin tolerance test after 10 weeks of diet: LFD groups (left panel, n= 3-6) and HFD groups (right panel, n= 7-8). There were 2 LFD mice excluded due to hypoglycemia during the insulin tolerance test.